RESPONSE OF MATERIALS TO IMPULSIVE LOADING

Hallock F. Swift, et al

Dayton University

Prepared for:

Air Force Materials Laboratory

May 1970

Unclassified
Security Classification

AD 783315

DOCUMENT CONTROL DATA - R & D

(Security classification of title, body of abstract and indexing annotation must be entered when the overall report is classified)

1 ORIGINATING ACTIVITY (Corporate author)
University of Dayton Research Institute
300 College Park Avenue
Dayton, Ohio 45409

2a. REPORT SECURITY CLASSIFICATION
Unclassified

2b. GROUP

3 REPORT TITLE
RESPONSE OF MATERIALS TO IMPULSIVE LOADING.

4 DESCRIPTIVE NOTES (Type of report and inclusive dates)
Technical Report

5 AUTHOR(S) (First name, middle initial, last name)
Hallock F. Swift, Diamantis D. Preonas, Paul W. Dueweke, and Robert S. Bertke

6 REPORT DATE	7a. TOTAL NO. OF PAGES	7b. NO. OF REFS
April 1970	76	99

8a. CONTRACT OR GRANT NO.	9a. ORIGINATOR'S REPORT NUMBER(S)
F33615-68-C-1138	UDRI-TR-70-18
b. PROJECT NO. 7360	
c. Task No. 736006	9b. OTHER REPORT NO(S): (Any other numbers that may be assigned this report) AFML-TR-70-135
d.	

10 DISTRIBUTION STATEMENT
This document has been approved for public release and sale; its distribution is unlimited.

11 SUPPLEMENTARY NOTES	12 SPONSORING MILITARY ACTIVITY
	Air Force Materials Laboratory Air Force Systems Command Wright-Patterson AFB, Ohio 45433

13 ABSTRACT

Fundamental and applied impact investigations have been carried out by the University of Dayton Research Institute for the Air Force Materials Laboratory during the past two years under Contract F33615-68-C-1138. The areas of principal effort were hypervelocity impact studies, investigations of ordnance velocity impacts and studies of materials response to planar shock waves. The hypervelocity impact studies produced a large volume of time-resolved data describing impacts into thin sheets and thick plates. Ordnance velocity investigations were applied to immediate Air Force problems involving the ballistic responses of present aircraft components and also provided insights into the ballistic responses of airframe structures and airborne armor. Electrically powered planar impact generators were used to establish the damage thresholds of homogeneous and composite materials when subjected to short-duration shock waves that simulate the environment experienced by reentry vehicles exposed to nuclear explosions. More fundamental studies of materials shock response were also initiated.

DD FORM 1 NOV 65 1473

Unclassified
Security Classification

NOTICES

When Government drawings, specifications, or other data are used for any purpose other than in connection with a definitely related Government procurement operation, the United States Government thereby incurs no responsibility nor any obligation whatsoever; and the fact that the Government may have formulated, furnished, or in any way supplied the said drawings, specifications, or other data, is not to be regarded by implication or otherwise as in any manner licensing the holder or any other person or corporation, or conveying any rights or permission to manufacture, use, or sell any patented invention that may in any way be related thereto.

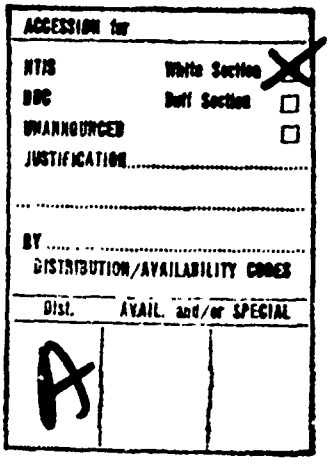

Copies of this report should not be returned unless return is required by security considerations, contractual obligations, or notice on a specific document.

14 KEY WORDS	LINK A		LINK B		LINK C	
	ROLE	WT	ROLE	WT	ROLE	WT
Impact Physics						
Hypervelocity						
Ordnance Velocity Impact						
One-Dimensional Impact						
Plate Slap						
Equation of State						
Photo Instrumentation						
Cloud Dissection						

ib

AFML-TR-70-135

RESPONSE OF MATERIALS TO IMPULSIVE LOADING

H. F. Swift
D. D. Preonas
P. W. Dueweke
R. S. Bertke
University of Dayton Research Institute

ic

FOREWORD

This document was prepared by the University of Dayton Research Institute, Dayton, Ohio, as a final report describing research carried out for the Air Force under Contract F33615-68-C-1138. The project was initiated under Project 7360: Chemical, Physical, and Thermodynamic Properties of Aircraft, Missile, and Spacecraft Materials, Task 763006: Impact Damage and Weapons Effects on Aerospace System Materials. The work was administered under the direction of Mr. Gordon H. Griffith of the Air Force Materials Laboratory, Air Force Systems Command, Wright-Patterson Air Force Base, Ohio. This report describes a completed effort but subsequent studies are being continued under Contract F33615-70-C-1228.

Several projects described in this report were carried out by students of the Air Force Institute of Technology as Masters and Ph. D. theses under the technical guidance and support of UD personnel. The names of these students are included in the text as their work is described. The authors wish to thank all the UD technical staff connected with this project without whose help the results described in this report could not have been achieved.

This report was submitted by the authors in April 1970. The University of Dayton report number is UDRI-TR-70-18.

This technical report has been reviewed and is approved.

Herbert M. Rosenberg

HERBERT M. ROSENBERG
Acting Chief, Exploratory Studies Branch
Materials Physics Division
Air Force Materials Laboratory

ABSTRACT

Fundamental and applied impact investigations have been carried out by the University of Dayton Research Institute for the Air Force Materials Laboratory during the past two years under Contract F33615-68-C-1138. The areas of principal effort were hypervelocity impact studies, investigations of ordnance velocity impacts and studies of materials response to planar shock waves. The hypervelocity impact studies produced a large volume of time-resolved data describing impacts into thin sheets and thick plates. Ordnance velocity investigations were applied to immediate Air Force problems involving the ballistic responses of present aircraft components and also provided insights into the ballistic responses of airframe structures and airborne armor. Electrically powered planar impact generators were used to establish the damage thresholds of homogeneous and composite materials when subjected to short-duration shock waves that simulate the environment experienced by reentry vehicles exposed to nuclear explosions. More fundamental studies of materials shock response were also initiated.

TABLE OF CONTENTS

Table of Contents (Continued)

LIST OF ILLUSTRATIONS

List of Illustrations (Continued)

List of Illustrations (Continued)

LIST OF TABLES

I. INTRODUCTION

The University of Dayton Research Institute has been engaged in a continuing study of impact phenomena under sponsorship of the Air Force Materials Laboratory for the past four years. The following is a final report describing the effort between 1 November 1967, and 1 April 1970, covered under Air Force Contract F33615-68-C-1138. During that period emphasis has been placed upon analyzing the responses of materials to hypervelocity impacts, ordnance velocity impacts, and impacts that produce planar "one-dimensional" shock disturbances.

Air Force systems that travel through near-Earth space are subject to a variety of macro-pellet impact hazards. The hypervelocity impact phase of the past and current effort has been aimed at evaluating magnitudes of impact hazards from both man-made and naturally-occurring particles and developing technology for protecting vehicles from them. Possible impact velocities range from below 3 km/sec to above 70 km/sec. Complete evaluation of the impact problem is impossible using direct laboratory simulation since currently available accelerators can launch pellets at maximum velocities of only 12 km/sec. Laboratory investigations of space impacts must, therefore, be carried out at sub-realistic velocities--a questionable procedure unless the studies are aimed primarily at obtaining fundamental understandings of hypervelocity impact processes which can be extrapolated reliably to realistic velocities.

The second area of study concerns impacts in the velocity range of current and future ordnance. It is aimed at evaluating gunfire and shrapnel threats to aircraft structures and measuring the performance of materials and structural designs used to reduce these threats. Actual field conditions for these impacts can be simulated closely in a laboratory; therefore, a large part of the effort has been placed upon evaluating the ballistic responses of aircraft materials, structural concepts, existing and proposed aircraft armor, and present aircraft components. More fundamental studies are also being carried out to develop a basic understanding of materials impact response in the ordnance velocity regime. The data from these studies is required to guide the development of future materials and structural concepts designed to minimize impact threats to future Air Force systems.

Components and structures of many Air Force systems may be subjected to shock loading during combat operations. Basic evaluation of systems reactions to these loadings requires knowledge of fundamental materials response to shock wave loading. The third phase of the impact response effort is aimed at providing such information by observing the response of flat-plate specimens to planar shock waves generated by

impacts with flat-faced projectiles. To date, the major emphasis of this effort has been to establish damage thresholds of reentry vehicle material samples to shock loading from impacts with very thin plastic sheets. These impacts produce loading profiles simulating those sustained by reentry vehicles under enemy attack. Recently, studies were initiated for gaining more fundamental knowledge of the shock responses of a wide range of materials.

II. HYPERVELOCITY IMPACT STUDIES

Hypervelocity impact experiments were conducted at the AFML hypervelocity impact facility[1] located in Building 56, Area B of Wright-Patterson AFB. The facility consists of a small light-gas gun capable of launching a wide variety of small pellets to maximum velocities near 10 km/sec, an evacuated ballistic range, and instrumentation systems for monitoring pellet velocity and integrity. In addition, high speed instrumentation including various framing and streaking cameras, flash x-ray equipment, and associated electronics are available as are a group of specially developed techniques for specific measurement tasks.

As stated above, Air Force information requirements concerning hypervelocity impacts cannot be achieved directly in the laboratory because of fundamental velocity limitations of present-day pellet accelerators. For this reason the hypervelocity impact studies have been concentrated heavily in areas that provide fundamental information about the nature of various types of impacts as opposed to technical evaluations of specific current and proposed protection techniques. These objectives have required that many of the individual studies rely upon dynamic measurements taken during the impact. Many instruments and measurement techniques were developed during this effort which provide the facility with unique dynamic measurement capabilities.

Background

At the time the AFML/UD effort began, a considerable body of information concerning the qualitative aspects of hypervelocity impact was available. Theoretical models had been proposed for such impacts that were quite plausible, but many significant details were recognized to be missing, largely because (1) materials response to dynamic loading was virtually unknown, and (2) little information concerning the dynamic aspects of hypervelocity impact processes was available. In spite of these limitations, several models were formalized into codes whose results, by virtue of their completeness, were widely held to be "reasonably accurate".

In addition, a truly vast amount of hypervelocity impact damage information was available. Various government agencies have financed from between 10,000 and 20,000 firings of a variety of projectiles into targets ranging from blocks of well-characterized homogeneous metal to actual components of space vehicles. Although several notable efforts had been made to codify these results[2, 3], the bulk of them were of little general use because of such factors as: essential experimental details were not reported; target materials were poorly characterized; and experiments were designed to yield information pertinent to only a single

engineering goal. On the basis of these studies, numerous papers have been written discussing empirical correlations of impact data[4, 5, 6]. The limitations described above resulted in significant disagreements between the various empirical formulations for predicting impact damage and those predicted by the computer codes.

The decision was made early in the AFML/UD effort to concern ourselves primarily with experiments specifically aimed at illuminating the nature of hypervelocity impact processes, and to use carefully characterized materials and procedures so that the resulting data would be the most efficient generated thus far both for engineering evaluations and for expanding understanding of the hypervelocity impact process.

The experimental program has been divided quite naturally into two phases: the study of impacts into thin plates which are punctured by the impact, and impacts into thick "semi-infinite" targets which are not punctured. Both studies provide fundamental information about hypervelocity impact processes that is needed for evaluating and guiding theoretical development. Significant progress has been made in these experimental programs prior to the current contract effort and this progress has been expanded at a rate well in excess of any achieved during earlier hypervelocity impact investigations.

THIN PLATE IMPACT STUDIES

Whipple proposed a scheme for protecting space vehicles against hypervelocity impacts that relies upon pellet impact with a thin sacrificial plate (bumper) spaced some distance from the vehicle hull to reduce incoming pellets to fine clouds of rapidly dispersing debris. The relatively diffuse impact of this debris upon the vehicle hull can be withstood much more easily than could the concentrated impact of a non-intercepted pellet. This protection concept has been studied widely at many facilities[7, 8, 9, 10], and is agreed to be the most effective one developed to date for protecting space vehicles. Accordingly, the study of such structures received much emphasis during the contract effort. Thin plate investigations have been divided between studies aimed at elucidating particular aspects of hypervelocity impacts into two-plate structures and those providing detailed dynamic analyses of specific impact situations that the authors feel possess special characteristics typical of those generated by impacts against actual space systems.

A. Bumper Materials Effects Studies

A study was carried out to investigate the relative performance of a range of bumper plate materials as established by ballistic limit evaluation[B2, B26]. A specific class of impact situations was chosen to: (1) reduce the total number of new data points to a minimum; and (2) to

provide maximum correlation with previous results obtained both here and elsewhere. Accordingly, the fixed parameters were: 0.317 cm diameter spherical projectiles of 2017 aluminum traveling at velocities between 6.9 and 7.3 km/sec; rear plates of 6061-T6 aluminum spaced 5.08 cm behind the bumper; and ballistic limit defined as the minimum thickness rear plate that would survive an impact without sustaining a gas leak. Bumper plates were made from 17 materials whose thicknesses were adjusted to provide a single areal density of 0.22 gm/cm^2. Figure 1 is a graphical presentation of overall results from this study.

These results indicate that: (1) the thermodynamic properties of the bumper and pellet materials alone determined bumper effectiveness; (2) bumper areal density was the only factor affecting performance when impact-induced shocks were sufficiently intense to melt both the pellet and bumper material involved in the impact; (3) similar constant-areal-density rules probably are applicable when the pellets melted but the bumper material either remained solid or vaporized; and (4) bumper performance degraded rapidly as material densities were reduced below 2 gm/cc. This effect was related to the fact that bumpers made from such materials fail to produce strong enough shock waves in the pellets to melt them so that, as the bumper densities dropped, progressively larger chunks of pellet material were allowed to pass through the bumpers and strike the rear plates.

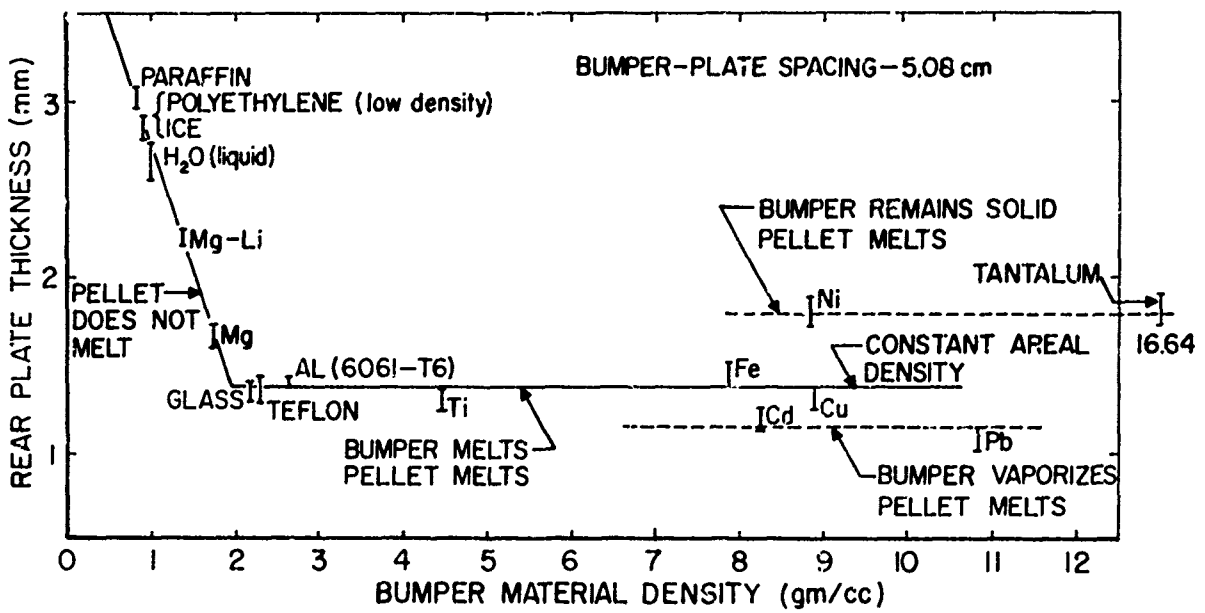

Figure 1. Results of Bumper Material Effects Study Showing States of Debris Material.

These results fill a specific gap in previous knowledge that had led to considerable controversy between competing techniques for estimating two-element shield performance. In addition, the study provides a serious warning about material density limitations for bumpers of space vehicle protection structures.

B. Hole Diameter and Hole Growth Studies

The final hole diameter in a thin plate struck by a hypervelocity pellet together with its rate of enlargement are of both fundamental and practical interest. Material thrust behind an impacted bumper plate from the immediate region of the hole determines the strength requirements for the rear plate of a two plate particle shield. Should the rear plate be perforated massively, the final diameter of the hole in the bumper plate will strongly effect the "blow down" rate of a vehicle interior. Of more fundamental significance is the fact that hypervelocity perforation of thin plates represents the most basic form of a hypervelocity impact since the material subjected to very high impact pressures is swept away from the target before these pressures drop to the point where material strength properties can affect the process. The remainder of the hole growth is simply the response of a thin plate to a strong shock directed radially outward from the impact point. Finally, the authors' attention was directed to the hole growth process by some data generated during work on an earlier contract which appears to show that holes in thin plates impacted by hypervelocity pellets expand to 130% of their final size while debris clouds are emitted and then shrink at some later time.

An experimental program was set up to use flash x-ray equipment for measuring hole diameter as a function of time after initial contact between the pellet and the plate*. Three impact situations were chosen: plates of aluminum, copper, and cadmium were impacted by spheres of the same material traveling at 7 km/sec (nominal). Sphere diameters were four times the thicknesses of the impacted plates. Additional experiments were carried out to observe the emanating points of the energetic debris emitted behind the plates; multiple impacts of these debris particles are responsible for almost all damage to the rear plates of two element particle shields. Experimental techniques employed for measuring these emanation points are described in Section II-D. Finally, hole diameters in approximately 400 plates impacted at this facility during the past four years were codified and the resulting information relating hole diameters to impact and plate parameters were compared with a sampling of widely used empirical data fitting expressions and predictions from numerical codes.

---

* The bulk of these studies were carried out with the support and guidance of the University by Capt. W C. Turpin as part of his Air Force Institute of Technology Master's Thesis (see Ref. B29).

Figure 2 is an example of the hole diameter versus time curves generated during these experiments. The following conclusions were drawn from the results of this study: (1) hole growth is a two stage process starting with a rapid initial growth and continuing much more slowly to the final size; (2) no measurable rebound of hole diameter was observed (experimental resolution was such that no rebound over 2.5% could escape observation); (3) the energetic material emitted behind an impacted plate comes from an area much smaller than the size of the final hole. In most cases, this area is only slightly larger than the projection of the impacting pellet upon the plate surface. Figure 3 is a composite plot relating final hole diameter for 6061-T6 aluminum plates to several ballistic parameters. None of the empirical expressions investigated[3, 5, 11] correctly predicted all the hole size data.

C. Velocity Scaling Studies

Experimental results from this facility and others indicate that the ballistic limit of two plate meteoroid shields varies only slightly with pellet velocity in the range of 6.5 to 7.5 km/sec. Indications are strong, however, that the limit thicknesses of the rear plates are significantly greater at both higher and lower impact velocities. Clearly, the energy content of the debris cloud behind a bumper plate will be increased as impact velocities are increased and hence will require a stronger second plate for successful containment. As impact velocities are lowered, incoming projectiles are not completely fragmented by the bumper impacts; thus relatively large pellet chunks impact the second plate. Many investigators believed that a single maximum ballistic limit thickness of the rear plate would be achieved as projectile velocities were lowered to a critical value[4]. Further velocity reductions would reduce the impulse of the incoming pellet to the point where the damage potential of its fragments would be reduced--regardless of their size. Eventually, the incoming pellet would be contained by the first plate. Figure 4 is a plot of rear plate thickness versus impact velocity for 0.318 cm aluminum spheres impacting 0.079 cm thick 6061-T6 aluminum plates with 6061-T6 aluminum rear plates spaced 5.08 cm behind. Note that the ballistic limit curves have substantial structure and that at least two rear plate thickness peaks are resolved. To date, no explanation is available for this curious behavior but further studies aimed at clearing up this anomaly are planned.

D. Debris Cloud Characterizing Experiment

The largest experiment carried out to date on the hypervelocity facility had, as its overall aim, the production of the most complete simulation of macropellet impacts upon actual space vehicles that can be carried out at this time. Computer models of thin plate impacts are in such an advanced state of development that they can make detailed predictions of debris cloud parameters generated by impacts at velocities typical of those encountered in space, i.e., well in excess of those

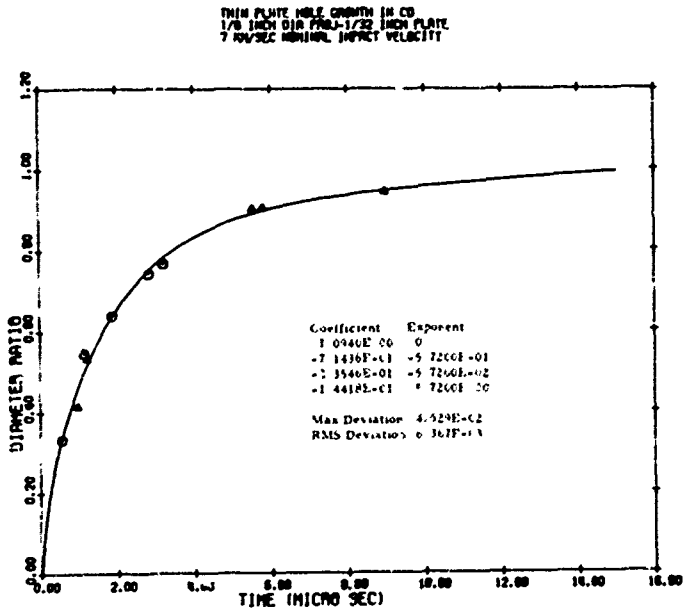

Figure 2. Hole Growth Rate in Cadmium (3.18 mm dia. Projectile, 0.85 mm Plate, 7 km/sec Impact Velocity).

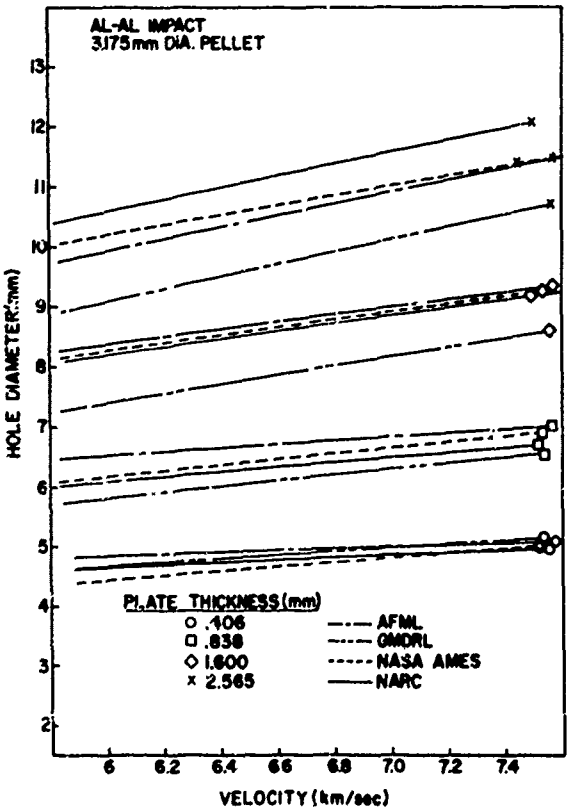

Figure 3. Hole Diameter vs. Velocity for 3.18 mm Aluminum Spheres Impacting 6061-T6 Aluminum Plates of Various Thickness.

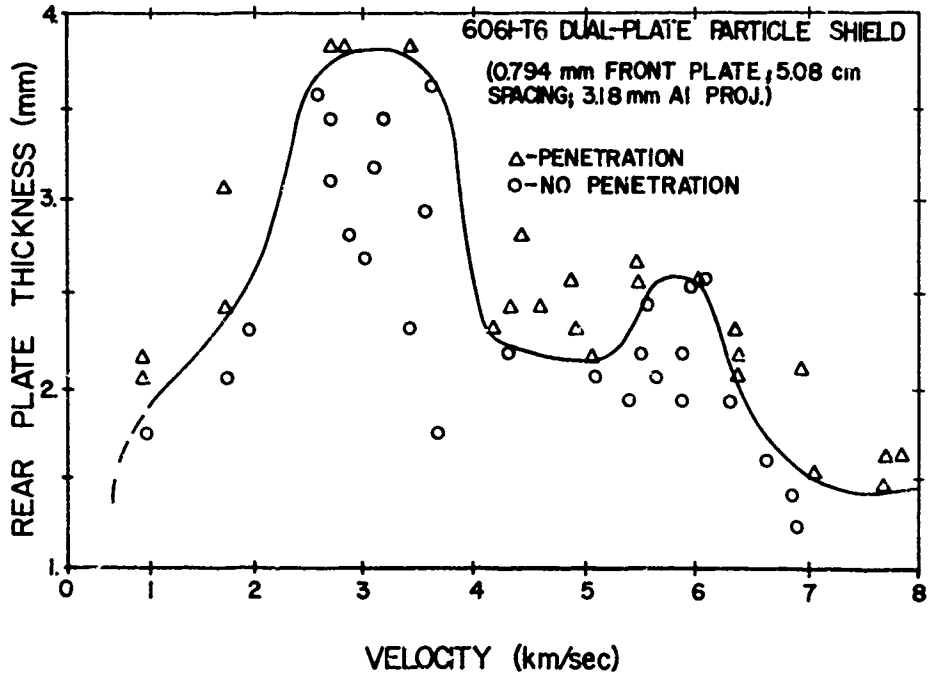

Figure 4. Ballistic Limit (Minimum Rear Plate Thickness) vs. Velocity for 6061-T6 Two-Plate Particle Shields Impacted by 3.18 mm Aluminum Spheres; 0.794 mm Front Plate is Spaced 5.08 cm From Rear Plate.

achievable in the laboratory. The assumptions inherent in these analyses become progressively more accurate as impact velocities are increased. Thus detailed descriptions of actual pellet encounters with bumper shields can be obtained. Theoretical techniques for predicting the responses of rear plates to impacts of diffuse debris clouds are in such early stages of development at this time that adequate response predictions are not available. Accordingly, UD proposed: (1) to employ impact codes to estimate the characteristics of debris clouds from actual pellet vehicle encounters; (2) to locate impact situations achievable in the laboratory which produce clouds with similar individual characteristics; and (3) to employ clouds from these impacts for evaluating the response of various rear plates and structures. In this way, the strong points of current experimental and theoretical techniques can be used to provide a hybrid simulation of actual impacts whose validity exceeds that of any other technique currently available.

Cronic divergences between computed impact predictions and similar experiments led the authors to conclude that it was necessary to check the validity of computer codes to be used in this effort. A code*

---

* The code was STEEP, a two-dimensional Eulerian code based on a hydrodynamic elastic-plastic model. It was developed by Shock Hydrodynamics Inc., Sherman Oaks, California and applied by them to this problem under Air Force Contract F33615-67-C-1712 (see Ref. 12).

was therefore applied to a selection of three impact situations that could be produced in the laboratory and that, together, possessed each of the characteristics expected for space encounters[12]. The three situations were the impacts at 7.5 km/sec of aluminum, copper, and cadmium spheres against plates of identical materials whose thicknesses were one quarter of the pellet diameters. Results from these computations were compared with experimental results from similar impacts. The following critical debris cloud parameters were chosen for comparison with code calculations: (1) material distribution within the cloud; (2) trajectories of selected cloud elements; (3) peak material velocity as a function of ejection angle; and (4) cloud impulse versus ejection angle. These parameters can be used together to determine cloud energy as a function of ejection angle and the total internal momentum of the cloud. Measurement of these parameters to reasonably high resolution represents a fundamental advance to the state-of-the-art of dynamic impact measurements. Each of them rely to one degree or another upon a fundamental technique for dissecting rapidly expanding debris clouds. Various applications of cloud dissection techniques plus experimental data to verify their general validity are presented in References B3 and B4.

Material Distribution

Observations of expanding debris clouds with high speed cameras and flash x-ray equipment have been carried out here[B3] and at a number of other facilities[7,8] (see Figure 5). There has been much speculation about whether these clouds are filled with material or are simply thin empty shells. A technique for dissecting debris clouds so that material distribution can be observed directly was developed*. Massive steel jaws were set to intercept expanding debris clouds so that only a slice of the cloud containing the original pellet trajectory could pass (see Figure 6). Flash x-rays taken of the cloud after subsequent expansion demonstrated that, for each of the cases observed, virtually all the cloud material was concentrated in a thin shell. One important consequence of the observed thin cloud shell is that virtually all cloud material projected at any particular angle leaves the impact area at a single time and travels at a single velocity. On the other hand, code predictions covering identical impacts indicated that the clouds were quite thick (see Figure 7). This disparity represents a fundamental divergence between predicted and observed results which cannot be explained by experimental error or code resolution.

---

* The first dissection experiments were designed with the support and guidance of the University by Capt. D. A. Carey and carried out as a portion of his Air Force Institute of Technology Master's Thesis (see Ref. 13).

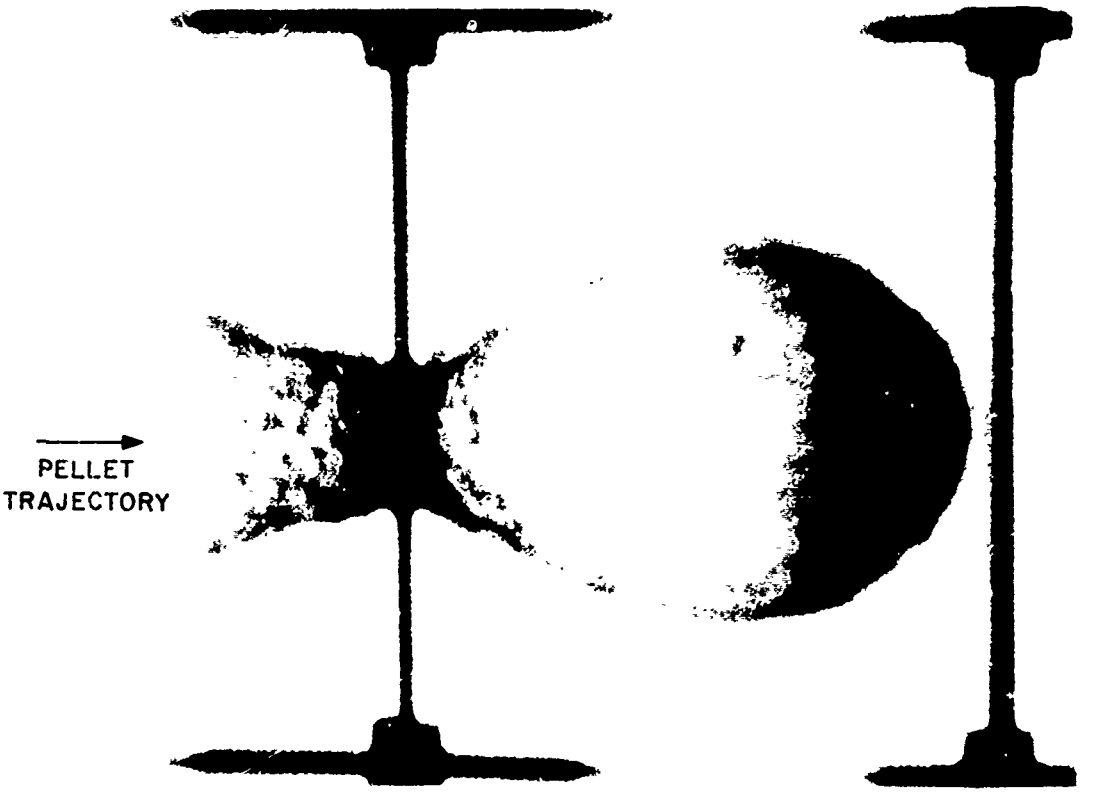

Figure 5. Debris Cloud From a Thin Plate Hypervelocity Impact.

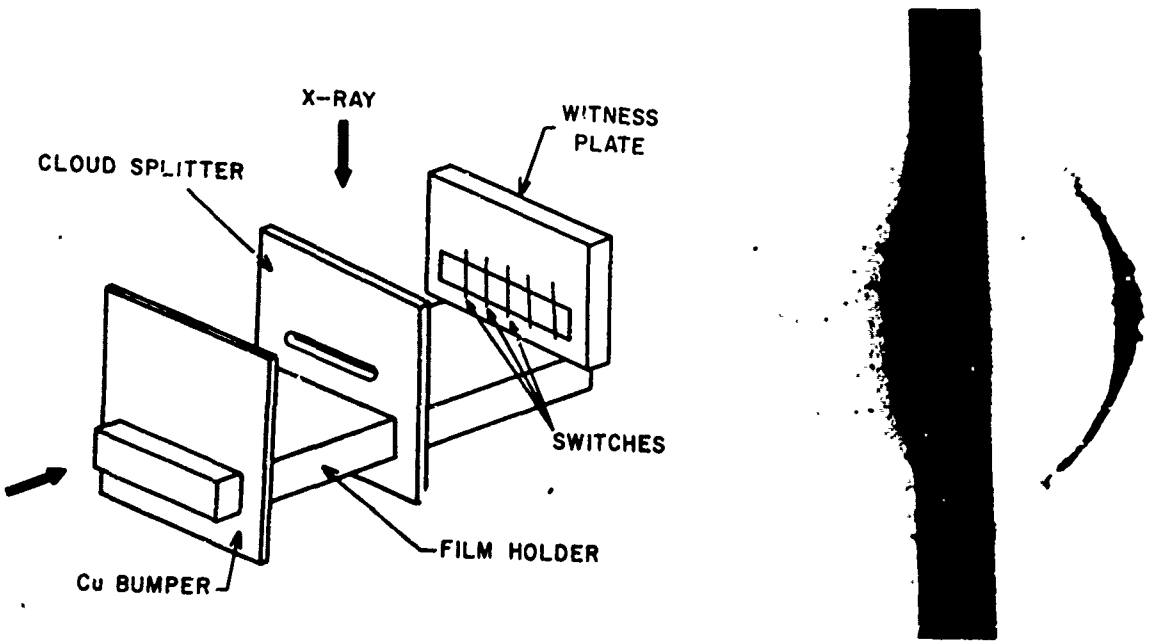

Figure 6. Experiment for Dissecting Debris Cloud to Determine Material Distribution.

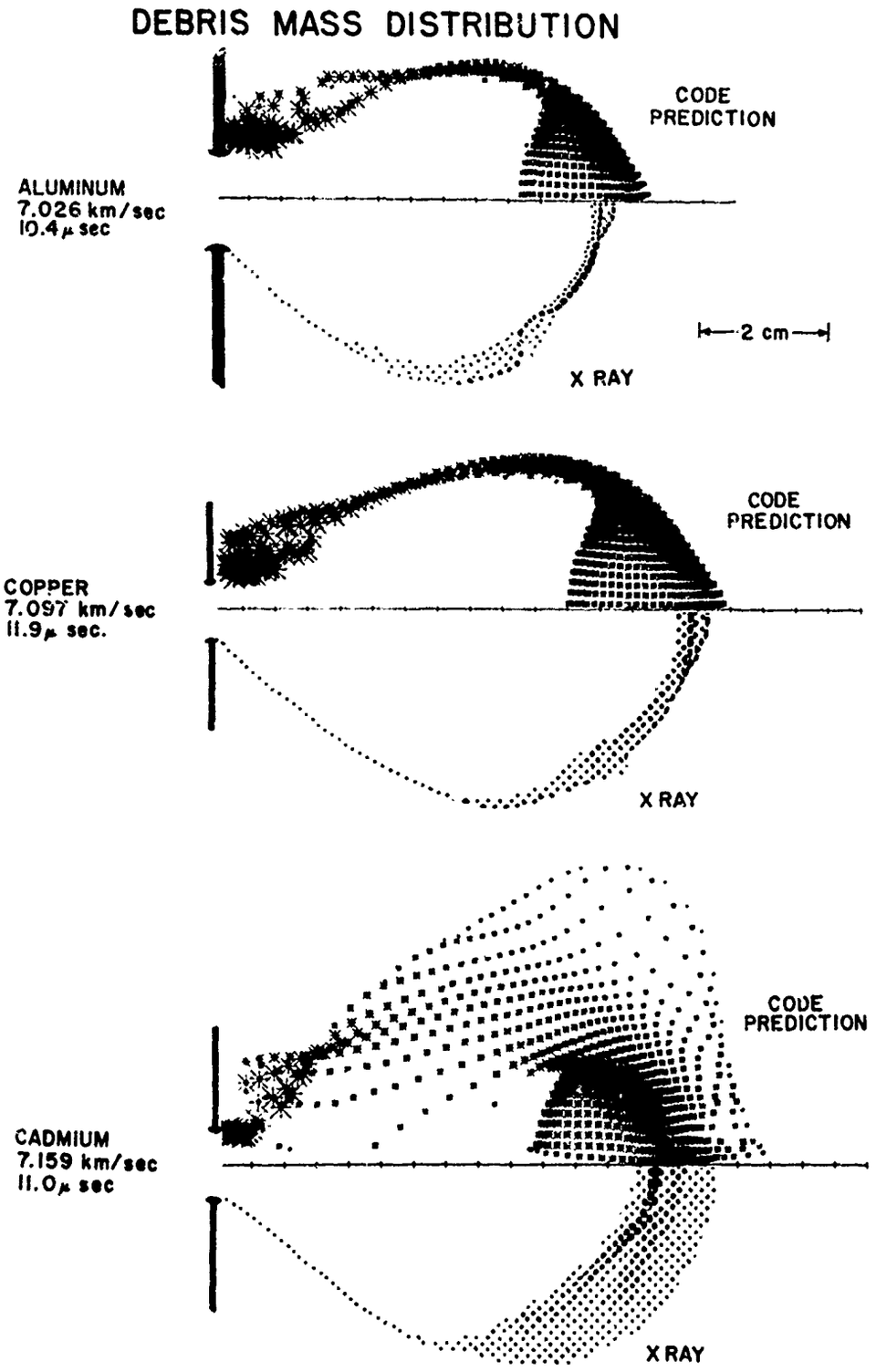

Figure 7. Comparisons of Observed Material Distributions of Debris Clouds With Computer Predictions.

Material Trajectory Study

The trajectories of cloud elements form a relatively sensitive check upon the validity of code predictions of hypervelocity impacts onto thin plates. These trajectories were measured by allowing a debris cloud expanding behind an impacted plate to intercept a precision grid of fine copper wires[B3]. The wires dispersed the material impacting them to the point where an image of the grid could be detected on the surface of a witness plate placed a known distance behind it (see Figure 8). Precisely-measured intersection points of the grid image were aligned with the positions of the original grid intersections and the resultant lines extrapolated to the region of the impacted plate. Trajectories of up to 100 cloud elements can be determined in this manner. Within the assumption that the debris elements travel in straight lines, these extrapolated lines represent trajectories of cloud debris elements. Careful experimental observations have demonstrated that this assumption is valid to within the resolution of the data. Results from a typical firing are presented in Figure 9. Note the large volume of useful data per shot that is achieved with this technique. The data demonstrates that energetic elements of impact-generated debris clouds are launched from a small area around the center of the final hole in the impact plate. Conversely, most of the expansion of such holes fails to produce significant debris. These conclusions are consistent with the observations of rapid initial hole growth rates and that the material ejected at particular angles travels at a single velocity. Within the two-dimensional limit of the computer analysis of the impact processes, the predicted results correspond with the measured ones. Unfortunately, the enforced two dimensionality of the analysis results in a relatively large uncertainty in the predicted radiating point of the material thus making a detailed comparison with experiments difficult.

Material Velocity Evaluation*

One of the most crucial parameters of an expanding debris cloud is its velocity profile. The measurement of velocity versus angle is unique, since the cloud is thin and all material traveling at particular angles travels at a single velocity. The most obvious technique for measuring cloud velocities is to photograph the clouds sequentially with a framing camera and perform conventional motion analysis. This approach is infeasible for expanding debris clouds because their surfaces are quite smooth so that individual points cannot be identified from frame to frame--thus cloud motion cannot be determined unambiguously. This

---

* The initial stages of this study were carried out with the support and guidance of the University by Capt. W. C. Turpin as part of his Air Force Institute of Technology Master's Thesis (see Ref. B29).

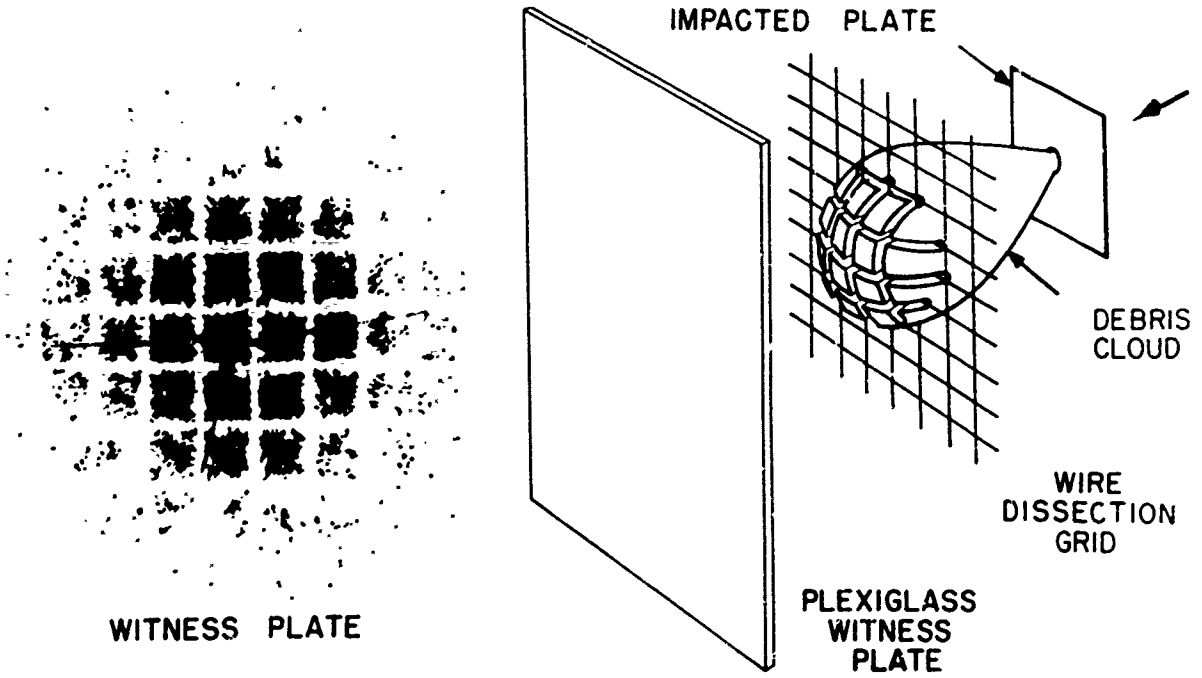

Figure 8. Dissection Experiment for Determining Material Trajectories.

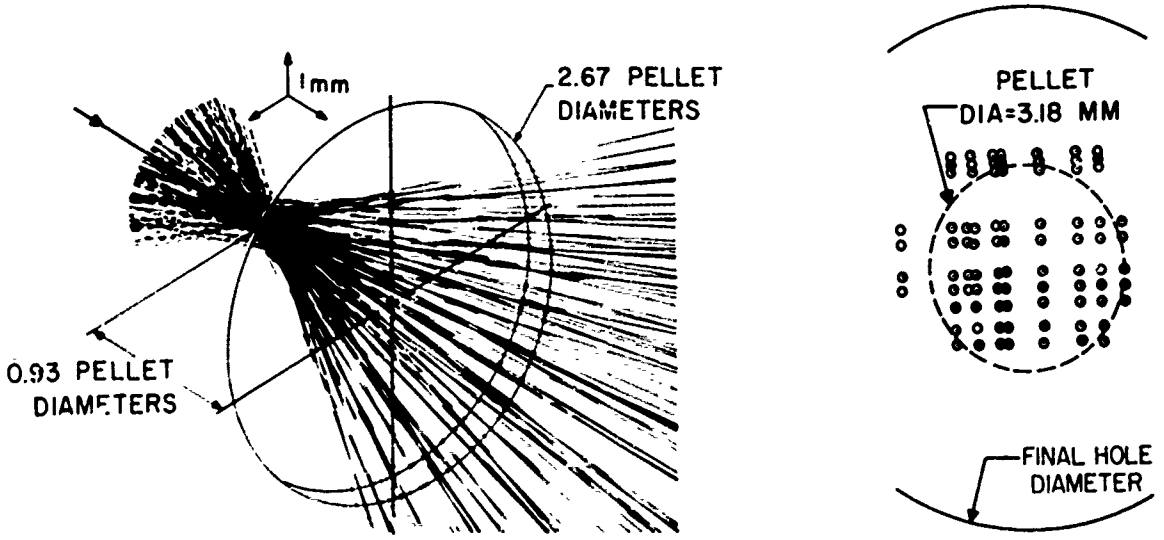

Figure 9. Isometric View of Material Trajectories for a Copper Plate Impacted by a Copper Sphere and the Intersections of the Trajectories With the Rear Surface of the Plate.

problem was first alleviated by allowing the cloud to intercept a massive plate with a row of small holes in it across the axis of the pellet trajectory[B29]. The holes allowed only individual segments of the cloud to pass whose velocities were then determined unambiguously from framing camera records. Relatively few data points (5-6 points per firing) were gathered with this configuration because of the relatively small number of holes that could be placed to intercept the cloud. A more advanced technique was developed that allowed as many as 20 velocity points per firing to be determined. A plate with a slot was used to intercept the cloud. Relatively fine wires were mounted across the slot to disperse small segments of the expanding cloud slice thereby "marking" it. Images of such a cloud configuration possess fine detail which can be interpreted readily. Figure 10 is a schematic of the velocity profile system together with some representative data and Figure 11 is a plot of cloud velocity versus angle off the original pellet axis for aluminum, copper, and cadmium impacts described above. The solid lines in these graphs are the code predictions for cloud velocity profiles. Note that they are at variance with the experimental results in each case and the correlation is particularly poor for cadmium (cadmium clouds are almost completely vaporized). Numerical difficulties in the initial problem setup distorted the code results within five degrees of pellet trajectory so that these variations should not be considered as representative of code malfunction.

Cloud Momentum Profile*

The momentum profile of an expanding debris cloud is one of the two most crucial parameters in determining its destructive potential to the rear plate of a two element particle shield (particle size distribution is the other). These profiles determine the overall loading of the rear plate and, together with cloud thickness measurements, provide an estimate of whether rear plates will fail via spallation. Cloud momentum is an especially difficult parameter to measure because any equipment making physical contact with the cloud distorts the measurements. This distortion arises because cloud material rebounds from any surface it contacts and, in extreme cases, craters or ablates the surface. The total momentum of the rebounded material (cloud and sensor) is measured as well as the internal impulse of the cloud. Two other factors tend to distort momentum measurements of intercepted clouds. Rebounding gaseous material stagnates near extensive surfaces and generates a long-duration pressure pulse whose total pressure-time history may produce significant impulse. On the other hand, when clouds are intercepted over

* The initial techniques for measuring cloud momentum were developed with the support and guidance of the University by Capt. J. H. Cunningham and applied by him as part of his Air Force Institute of Technology Master's Thesis (see Ref. B22).

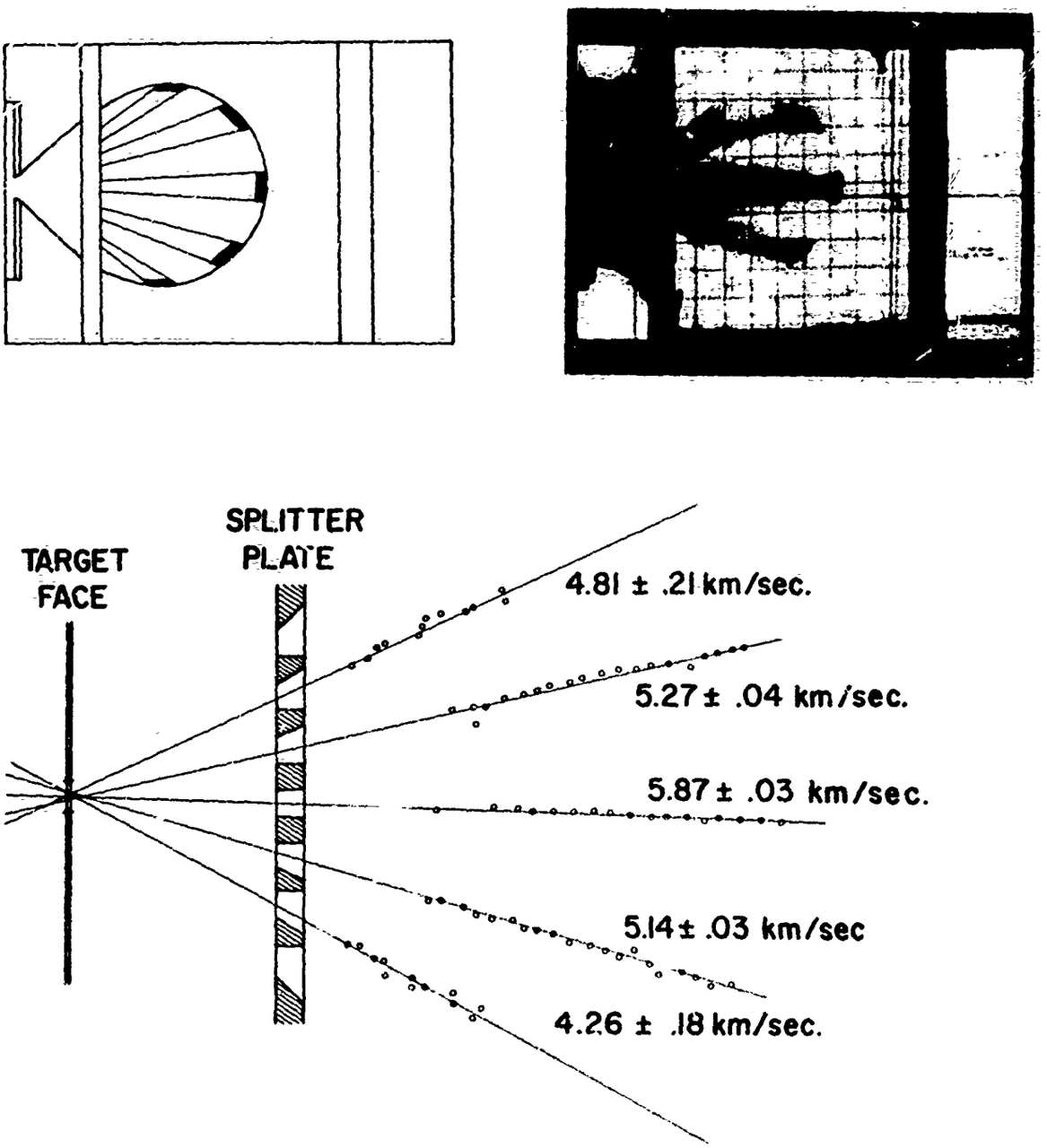

Figure 10. Dissection Experiment for Determining Velocity Profiles Using a Dissection Plate With a Row of Holes.

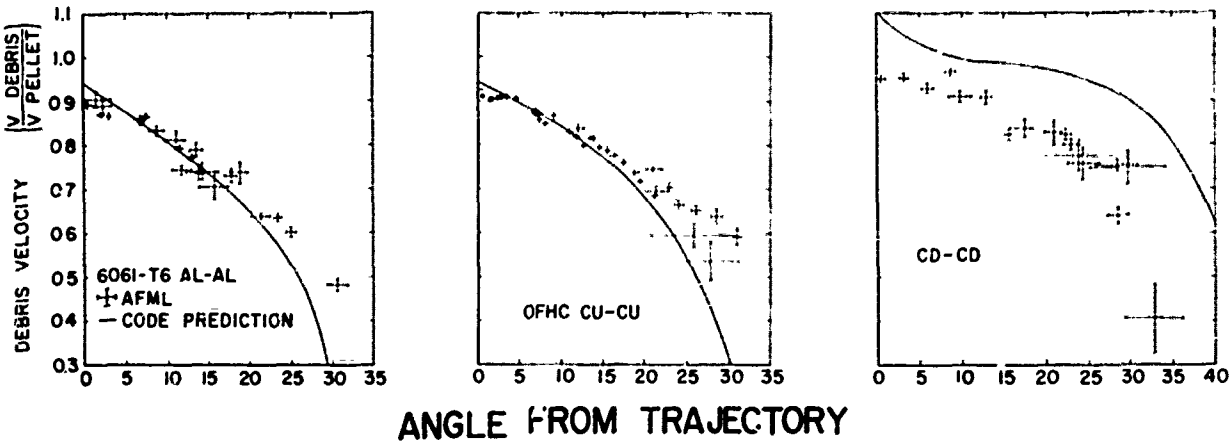

Figure 11. Material Velocity vs. Angle Off Trajectory for Debris Clouds Behind Aluminum, Copper, and Cadmium Plates Impacted by Spheres of the Same Material.

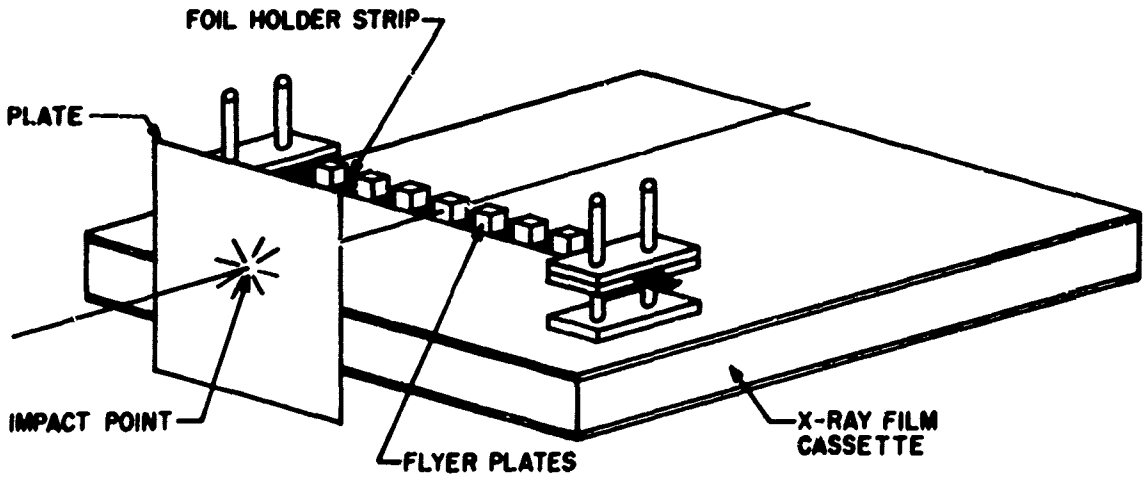

Figure 12. Experiment for Determining Debris Cloud Momentum Profiles by Observing the Motion of Freely-Suspended Flyer Plates Exposed to the Cloud.

small areas, flow fields are generated that divert part of the incoming material without bringing it to rest so that its full impulse is not sensed.

The fundamental technique adapted for measuring cloud momentum profiles was to allow the cloud to impinge upon an array of small metal plates mounted at known positions with respect to the impact point[B22] (see Figure 12). The recoil velocities of these plates provides a direct measure of the impulses they felt. Plate areal densities were adjusted to achieve recoil velocities between 5 and 200 m/sec. These velocities were low enough compared to the cloud velocities that: (1) impulse loading approximations could be applied safely; and (2) the plate velocities could be measured with a low-speed framing camera at times long after the debris cloud has been dissipated. A series of experiments was carried out for each of the three standard impacts described above. For each case, two separate experiments were run; first the plates were mounted freely so that a minimum amount of the cloud was intercepted, and then similar plates were mounted within holes in larger solid plates that completely intercepted the expanding clouds. No systematic deviations between these two methods for collecting data could be observed for any of the impacts. This lack of deviation has been interpreted as showing that the cloud impulse measurements were not disturbed by gas-dynamic stagnation or by flow fields established around the plates. The impulse profiles presented in Figure 13 are, therefore, accurate presentations of total cloud impulse plus any systematic rebound. A line of argument is presented in Reference 14 which indicates that rebound impulse is probably very minor and must be less than 25% in the worst case.

The solid lines on the graphs presented in Figure 13 are the predictions from the omputer code. At large angles they lie slightly below experimental values which can be justified on the basis of rebound momentum in the experimental measurements. With decreasing angle from the cloud axis, the predicted impulse intensities pass through maxima and then drop off while the experimental results rise monotonically. This qualitative difference in behavior is extremely significant because it leads to gross variations between experiment and theory at small angles off the cloud axis where all investigators agree that rear plate damage is most critical. One last point concerning this data bares mentioning. The data for the aluminum and copper impacts have relatively large scatter that cannot be explained by measurement imprecision (the RMS deviation of the angle and impulse measurements are within the size of the data points in almost all cases). The authors interpret this anomalous scatter as being caused by the particulate nature of the debris clouds. Previous studies have indicated that debris clouds behind copper and aluminum targets are made up primarily of solid chunks and liquid droplets. Each impulse sensing plate was struck by a finite number of particles and statistical variation in these numbers are postulated to have led to the anomalous scatter. The individual impact hypothesis is supported strongly by the fact that most of

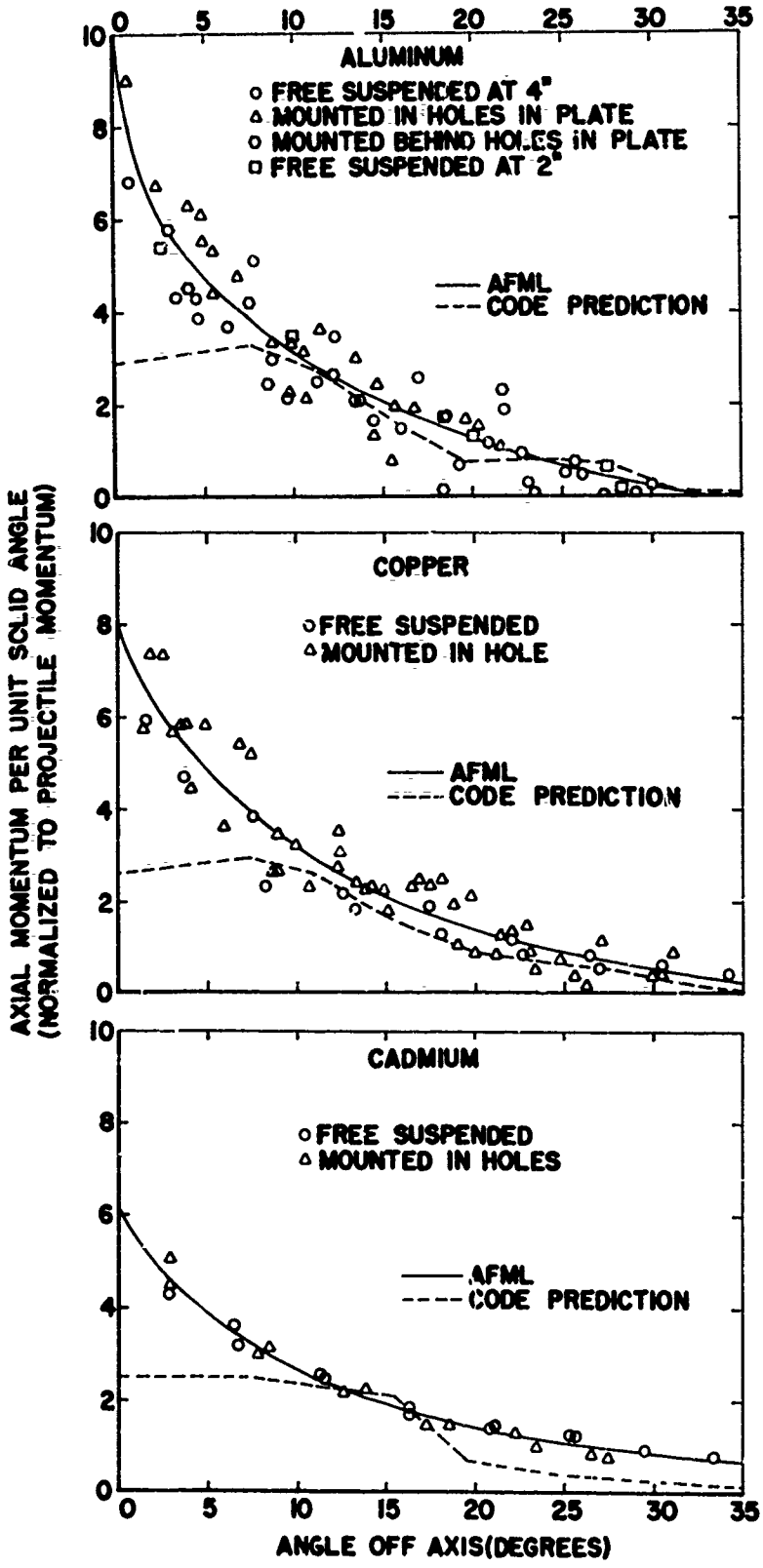

Figure 13. Momentum Profiles of Debris Clouds Behind Aluminum, Copper, and Cadmium Plates Impacted by Spheres of the Same Material. Computed Predictions Are Superimposed for Comparison.

the anomalous scatter disappeared from the impulse profiles behind the vaporous cadmium targets.

Dissection Validation and Discussion

Comparisons of computer predictions with experimental observations were so disturbing that they call into question either the validity of code predictions at any impact velocity or the reliability of the testing techniques. Accordingly, a study was initiated to check the reliability of the fundamental cloud dissection techniques used to gather virtually all the cloud characteristics data. Experiments were devised to observe dissection processes directly and to correlate measurements between dissected and undissected clouds. Figure 14 is a schematic diagram of one of the setups used to observe cloud dissection. The results indicated that dissection techniques were valid in all cases in which the data was used for code evaluation and also delineated conditions under which dissection techniques are inapplicable[B4].

The results of the dissection verification experiments have led the authors to believe that the experimental cloud characterization data is at least qualitatively accurate and therefore that the code has failed grossly to predict cloud characteristics accurately. The computer code chosen for this study[12] is typical of the best currently available numerical

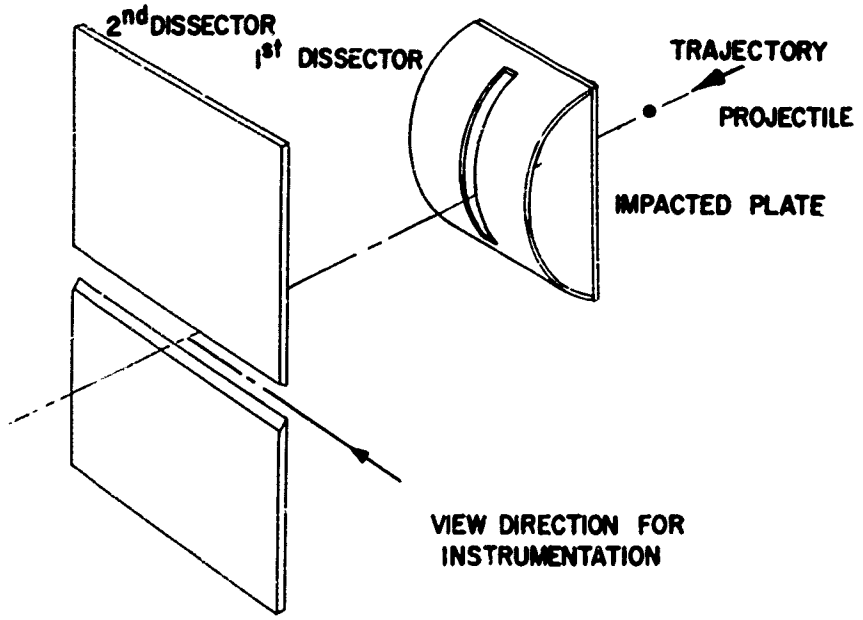

Figure 14. Dual-Dissection Experiment for Analyzing the Cloud Dissection Process.

technique for evaluating hypervelocity impacts. Therefore its failure to predict cloud characteristics must be viewed as a warning against using any computer-predicted hypervelocity impact results without thorough experimental verification.

The cloud characterization experiments described in the last four sections were carried out for the dual purpose of verifying the computer code model to be used for establishing debris cloud characteristics and to perfect experimental techniques for evaluating laboratory-generated debris clouds used to simulate space encounters. Because of the qualitative failures of the computer code, the emphasis of the program to simulate actual macro-particle encounters in space has been shifted to more fundamental analyses of the thin plate impact problem plus the development of more dynamic experimental results specifically aimed at providing data for further development of hypervelocity impact codes.

THICK PLATE STUDIES

The failure of computer codes to predict thin target impact phenomena has dramatized a long-standing need for studying hypervelocity impacts into thick plates. Impacts into thick targets are fundamentally more complicated processes than their thin plate counterparts because shock pressures range from pressures high enough to make metals flow freely to pressures well within the elastic limit of the target. Modern analyses based upon numerical solution of fundamental kinematic equations and equations describing dynamic materials response can be solved rigorously in regimes where target strength is unimportant. At lower pressure regimes that occur deeper into the targets, the equations become vastly more complicated because target strength becomes significant and finally dominates the impact process. Computations of all pressure regimes require detailed knowledge of target materials response to very high loading rates. Such information is almost completely unavailable.

To date, the bulk of code verification studies have consisted of comparing code predictions of final target damage with results from laboratory impacts. This procedure is inadequate for evaluating impact code performances since small differences between experiments and predictions will always exist. These differences must be interpreted as being either due to minor numerical and experimental inaccuracies or indicative of fundamental divergences between computer predictions and reality. The only adequate method for evaluating code validity is to check detailed predictions of impact processes against time-resolved results from dynamic impact experiments. In this way, the origins of any divergences between predictions and experiments can be traced and their importances evaluated. Hence a program was initiated whose ultimate goal was to acquire a wide base of fundamental dynamic data for a variety of hypervelocity impact situations which could be used both to evaluate numerical impact code performance and to guide the future development of these codes.

Preliminary Feasibility Studies

The initial effort in this area was to employ available flash radiographic equipment to observe crater growth profiles in thick aluminum targets impacted by aluminum spheres traveling at near 7 km/sec*. Four 300 kV flash x-ray generators were mounted in a single plane that contained the front surface of the target. Lead masks were arranged so that each x-ray generator exposed a film mounted behind the impacted target. The generators were triggered sequentially at preselected times after the projectile contacted the target. Figure 15 is a plot of normalized crater diameter versus time after impact. It indicates a monotonic increase of crater diameter as time progresses until the final diameter is reached. A supplemental experiment was aimed at determining whether equivalent crater growth data could be gathered from analyses of the debris plumes ejected from impact craters. The experiment failed because no dimension of the actual crater is mirrored in the plume geometry and no general technique for relating the two quantities could be found. The failure of this attempt demonstrates that the relatively large amount of crater

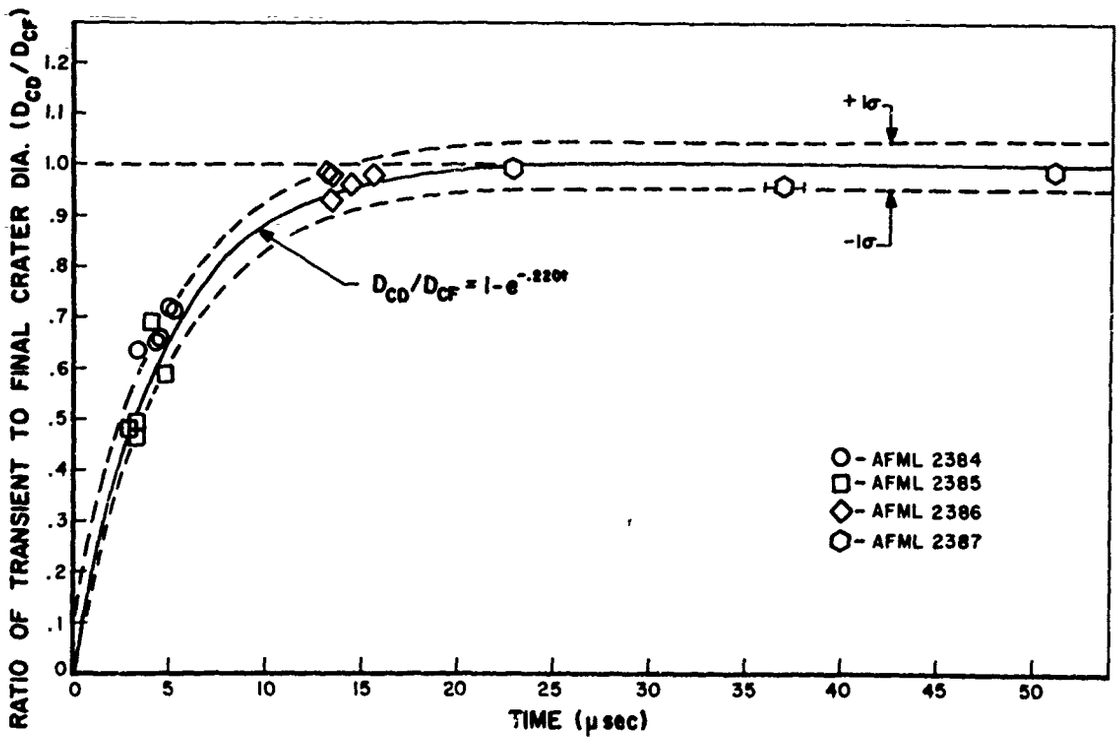

Figure 15. Crater Growth in 1100-0 Aluminum Impacted by Aluminum Spheres at 7 km/sec.

* This initial program was carried out with support and guidance from the University by Lt. Col. R. H. Smith as part of his Air Force Institute of Technology Master's Thesis (see Ref. B23).

growth data determined by ejecta plume analyses[15] is incorrect. The most important result of these experiments was that information concerning hypervelocity impact dynamics could be gathered with equipment at the AFML hypervelocity impact facility. Accordingly, a much larger experimental program was devised that would provide an initial data base against which the predictions of current and future impact codes could be measured.

Expanded Measurements of Thick Target Impact Parameters

An experiment was designed with the technical support and guidance of the University by Major R. F. Prater of AFML as his Ph.D. thesis effort to determine the following parameters for a number of hypervelocity impact situations: (1) crater growth rate; (2) peak shock pressure profiles; and (3) shock trajectories. The impact situations (tabulated in Table I) were chosen both to provide a broad data base for code comparisons and to elucidate

Table I

Thick Target Impacts Investigated

Nominal Projectile Velocity (km/sec)	Targets--Aluminum Alloy			
	1100-0	6061-T6	7075-T0	7075-T6
7.0	PST-A6.35 CG-A3.18 CG-A6.35 NC-A6.35	PST-A6.35 CG-A6.35	CG-A3.18	PST-A6.35 CG-A3.18 CG-A6.35 NC-A6.35
5.2	CG-A3.18	CG-S4.58	-	-
4.0	CG-A6.35 NC-A6.35	-	-	-
2.3	CG-A3.18	-	-	-

PST -- Pressure and Shock Trajectory Study.
CG -- Crater Growth Study.
NC -- Numerical Calculations.
A 2017 Aluminum (A) or Steel (S) Projectile Material.
S Number following is projectile diameter in millimeters.

the role of target strength in hypervelocity impact processes. Attention was confined to impacts between aluminum projectiles and various alloy aluminum targets whose static strengths varied from 0.9 kb for 1100-0 aluminum targets to 5.2 kb for the 7075-T6 aluminum targets[B25]. A refined version of the flash x-ray method used for the original crater growth study was chosen for measuring the sizes of evolving craters at specific times during their formations. Adapted versions of classical technique for monitoring surface motions were employed to determine the peak shock pressures in impacted targets; and both conventional and exotic shock sensors were used to determine shock trajectories.

A. Crater Growth Studies

In addition to the four 300 kV flash x-ray generators used for the initial crater growth study, six more lower voltage units were employed to take radiographs of the evolving craters along axes nearly parallel to the original pellet trajectory (see Figure 16). These six together with the four original units allowed a total of ten data points per firing to be generated (four provided both crater depth and diameter measurements; six provided only crater diameter determinations). Practical difficulties limited typical firings to seven to eight effective data points. Overall technique upgrading which included development of superior methods for measuring

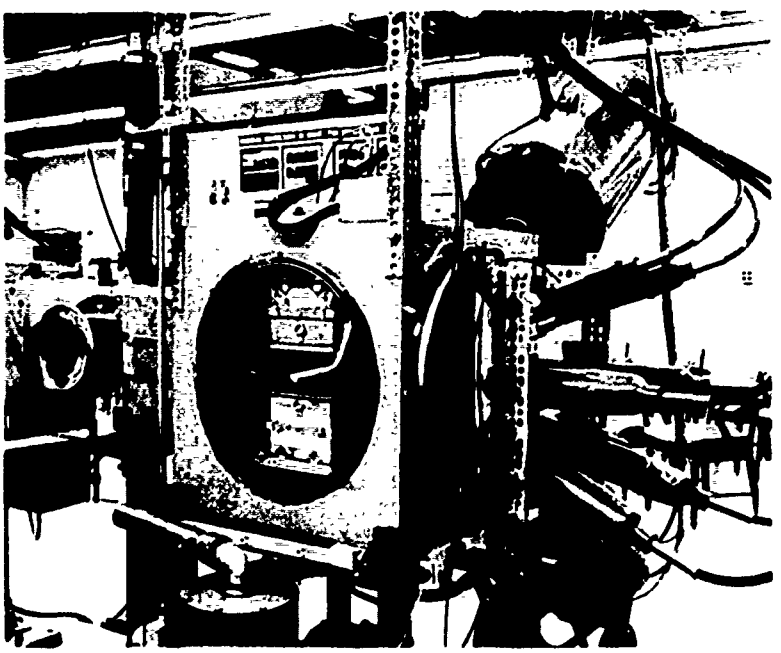

Figure 16. Experimental Setup for Determining Crater Growth.

x-ray films and better x-ray framing time determinations resulted in substantial increases in both quality and quantity of the x-ray data over the achievements of the initial study. Figure 17 presents results from a typical firing sequence. Again, the monotonic increase of crater size to its final value is observed. Curves of absolute crater size versus time for four strength aluminum alloys are presented in Figure 18. Note that the three curves are essentially identical at early times when pressures are so high that target strength is insignificant and that first the strongest and last the weakest alloy arrests crater growth. In no case was significant crater rebound observed.

Several years ago Gehring[15] presented crater growth data that showed 30% rebound of the crater during the growth process--a result which has caused much discussion ever since. The identical experiment was conducted as part of this crater growth study and the results are presented in Figure 17 together with Gehring's original data. Note that no rebound is observed and that Gehring's results are almost certainly in error. The authors wish to make clear that they infer no criticism of Gehring's original work. It was carried out at a time when flash x-ray instrumentation was in its infancy and, hence, represents a truly pioneering study.

In conclusion, the qualitative aspects of the study described present no contradiction to current thinking about hypervelocity impact phenomena. They do represent by far the most complete and accurate crater growth information ever compiled and, as such, will be invaluable for evaluating impact theories.

B. Shock Pressure Studies

Profiles of peak shock pressure are at least as sensitive indicators of code performance as are crater growth profiles. They have an additional advantage that they can be followed beyond the final crater surface into regions of the target that do not experience the extreme pressures generated near the impact point. Finally, a group of analytical theories for describing hypervelocity impacts as self-similar processes are available which treat shock propagation in some detail but can only treat crater growth in the grossest sense. Further development of these theories (possibly stimulated by comparison with the reported experimental data) opens the possibility that analytical techniques will be developed for predicting hypervelocity impact results with some reliability.

Very limited measurements of shock pressure profiles caused by hypervelocity impacts have been carried out by other investigators prior to this study. Charest[16] measured the recoil velocities of target rear surfaces opposite the impact point for a series of nominally identical hypervelocity impacts of aluminum spheres into various thicknesses of

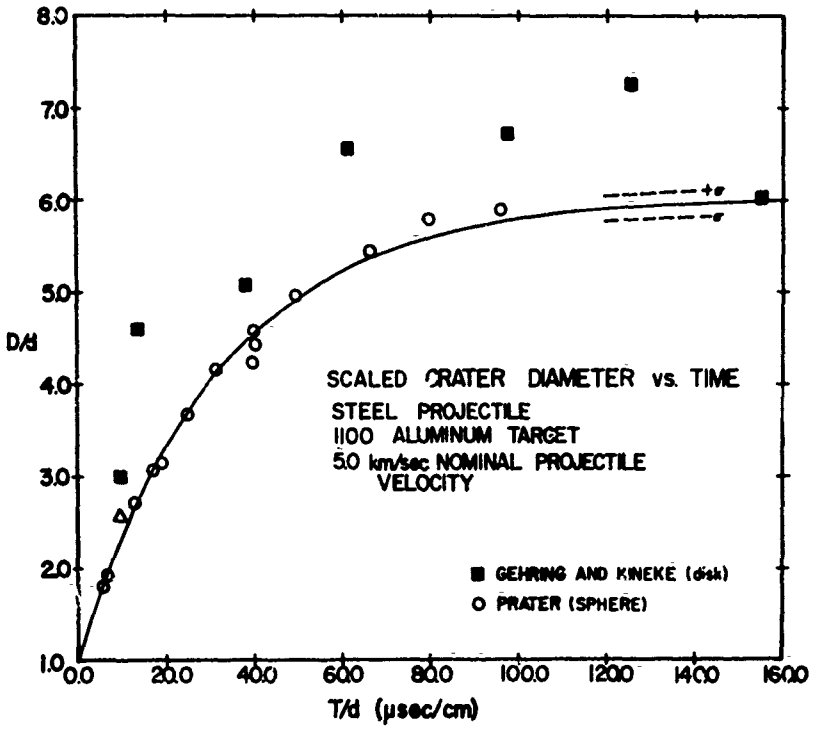

Figure 17. Typical Crater Diameter Growth Results Normalized to Projectile Diameter.

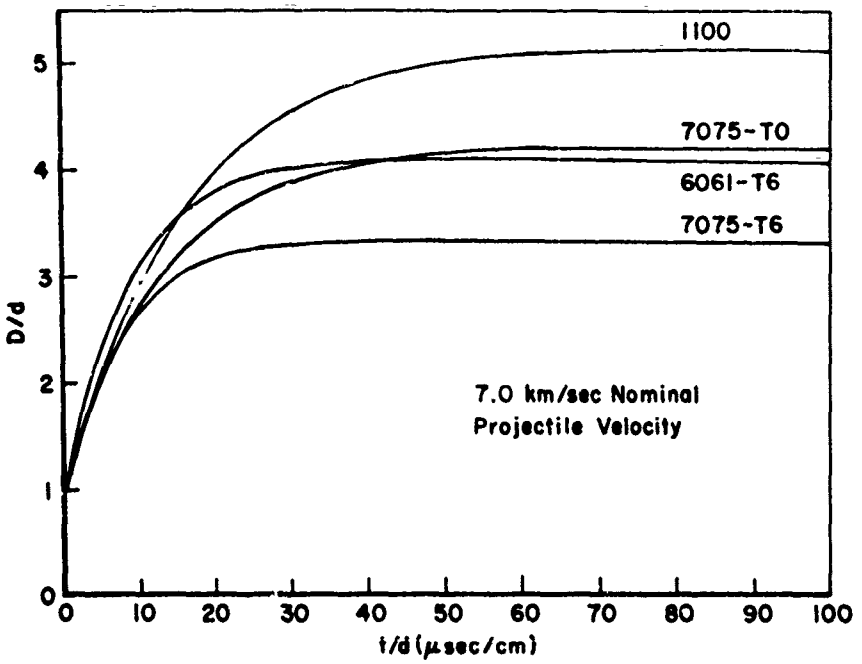

Figure 18. Comparison of Crater Depth Growth in Four Aluminum Alloys Normalized to Projectile Diameter.

1100-0 aluminum plates. High recoil velocities were measured directly with a high-speed framing camera. At lower recoil velocities, Charest placed thin plates of target material (fly-off plates) on the rear surface to store the peak recoil velocity; a medium speed framing camera monitored these plate velocities. He employed fundamental shock jump conditions, the widely used assumption that surface recoil velocity is twice the material velocity*, and the shock adiabat (Hugoniot) of aluminum to transform the recoil velocities to peak shock pressures. Billingsly[17] employed similar techniques to evaluate on-axis hypervelocity impact pressure profiles for a variety of homogeneous metals. Unfortunately, at low recoil velocities, he did not use fly-off plates to store the peak recoil velocity to assure that material strength effects did not retard the rear surface motion. Thus, his data for the low pressure portions of each pressure profile is highly suspect. Major Prater followed Charest's methods and related peak recoil velocity to peak shock pressures.

Prater concluded that to investigate the role target strength has in hypervelocity impact processes, shock pressure data was needed for a series of aluminum alloys whose strengths varied over as wide a range as possible. In addition, he felt that peak pressure information was needed at all points in the target rather than simply along the axis of symmetry. A strategy was adapted of impacting half cylinders on the center of their flat faces as is shown schematically in Figure 19. The nearly spherical shock wave radiating from the impact point strikes all points along a band of the cylindrical surface opposite the impact point almost simultaneously and normally. The motion of these elements of the rear surface are controlled by the peak shock pressures along the surface (i.e., at a single radial distance from the impact but at all angles between 0^{o} and 90^{o} from the original pellet trajectory). The radial dependence of shock pressure at all angles from the pellet trajectory is then determined by subjecting various diameter hemi-cylinders to nominally identical impacts and observing surface motion. A high-speed framing camera (Beckman & Whitley Model 300) was used to observe rear surface motions of a target setup shown in Figure 20. Initial firings demonstrated that the expanding target surface was smooth so that no information concerning directions of material motion was available. A system of wires was installed to intercept the expanding cloud and "notch" its surface. The subsequent motion of the notched target surface was used to determine that the surface material traveled perpendicular to the original surface under all circumstances--even when the original impact did not occur exactly on the hemi-cylinder axis.

As shock pressures were evaluated at larger distances from the impact point, peak shock pressures deminished to the point where target

---

* For aluminum this approximation has been shown to be valid within 3% for shock pressures up to 500 kbar.

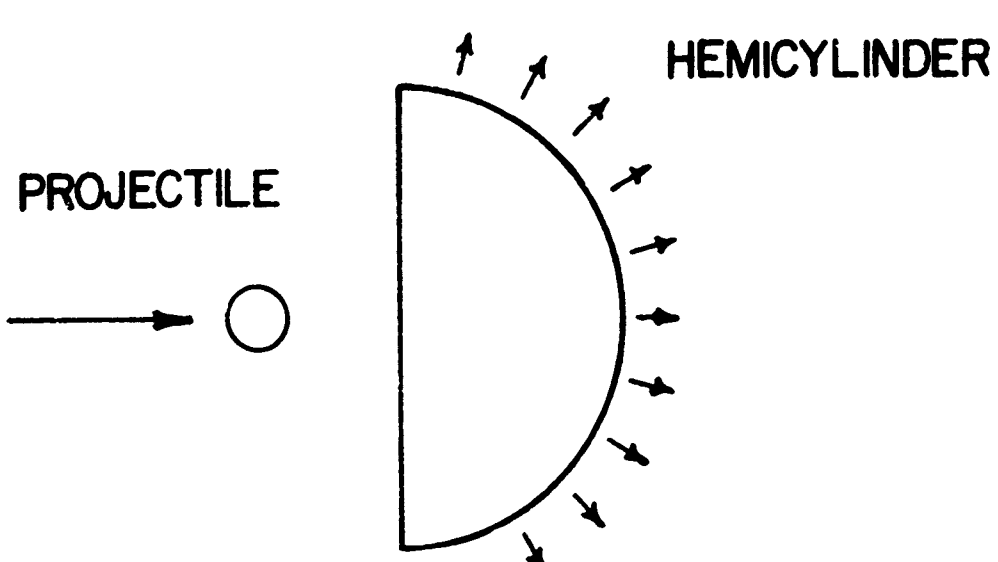

Figure 19. Hemi-Cylinder Experiment.

Figure 20. Hemi-Cylinder Experimental Setup Showing Debris "Notching" Wires.

strength effects decelerated the surfaces. Consequently, the cylindrical surfaces were flattened at selected angles to allow velocity measurement pellets to be attached. Again, these pellets recoil with the surface and maintain the peak surface velocity. Motion of the pellets was followed with either the B&W 300 camera or the B&W Model 326B Dynafax framing camera depending upon their velocities. In each case, the peak shock pressure at a single radius and five different angles from the axis of symmetry was determined. Progressively larger targets of this design were impacted until pellet velocity measurements revealed that the peak shock pressure was well below the elastic strength of the target materials.

The combined data from these two experimental setups yielded peak shock pressures at all points within the impacted targets, from points within the resulting crater, to points where the shock wave decayed into an elastic disturbance. Table I(p. 23) shows the impact situations that were analyzed in this manner.

Typical results from the peak shock wave pressure study are presented in Figure 21. In each case studied, the data could be fit best with two relationships shown as straight lines on the log-log plot of Figure 21. The slope of the early-time data (at small distances into the target) was found to be virtually identical for all aluminum alloys considered as was the slope of the late time data (with somewhat less precision). The point at which the slope change occurs is material sensitive and appears to correlate at least roughly with material tensile strength. A surprising fact is that the absolute pressures where these slope changes occur are far in excess of any strengths that have ever been associated with the aluminum alloys. At angles less than 30 degrees to the axis of symmetry, no angular dependence of peak pressure was observed. Pressures fell monotonically with increasing angles at angles between 30 and 90 degrees. These reductions of peak pressure with angle have been tentatively attributed to the interaction of pressure release waves emanating from the front target surface with the primary shock waves.

C. Shock Trajectory Studies

A secondary investigation was performed during the shock profile measurements to establish the trajectories (velocity histories) of the shock waves generated by the hypervelocity impacts. Velocity profiles of these waves can be related both to their peak pressure profiles and their pressure-time histories. Measurements of shock trajectories are complicated by the fact that, over a considerable pressure span, the waves possess a structured leading edge. This structure is developed at pressures below approximately 200 kb because the plastic component of shock waves(whose amplitude exceeds material strength)travels at subsonic velocity while the elastic disturbance(whose pressure approximates the dynamic yield strength of the material)propagates at local sonic velocity

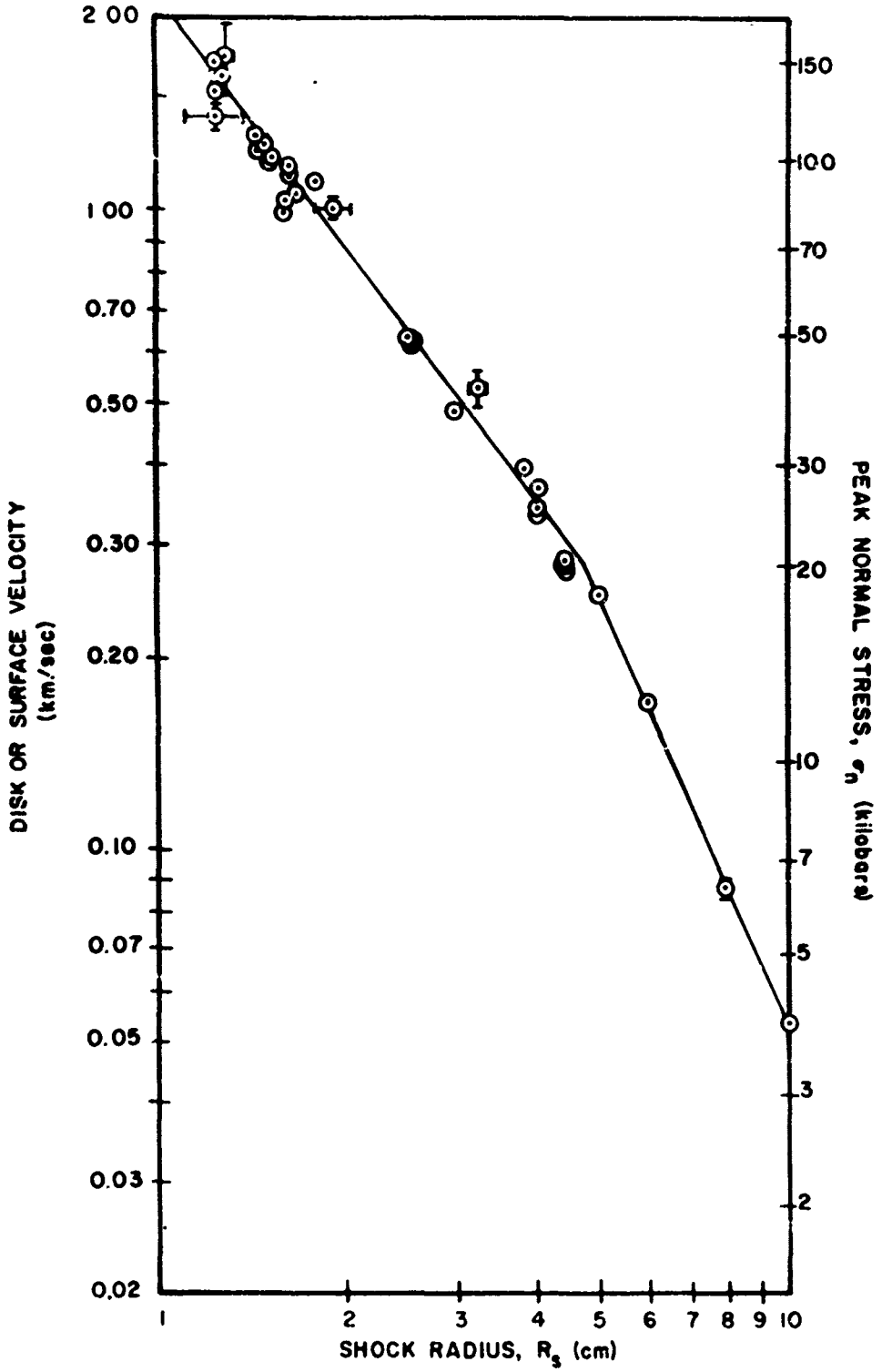

Figure 21. Typical Results of Peak Shock Wave Pressure Experiments Showing Peak Pressure vs. Depth Into Target for 1100 Aluminum Targets.

and thus moves ahead of the plastic wave. At relatively large depths into the target, the plastic wave is dissipated completely leaving an elastic disturbance with a single leading edge.

Three experimental techniques were developed for measuring the shock arrival times at different depths and angles in the impacted targets. Specially designed electrical pin switches described in Section V were used to measure shock arrival times when wave amplitudes above 200 kb were anticipated. Quartz piezoelectric gauges (see Section V) were employed to measure shock arrival times when shock pressures lower than 200 kb (and hence structured wave fronts) were anticipated. Their voltage outputs provide qualitative time histories of shock pressures viewed with high-speed oscilloscopes. The pressure versus time results resolve the elastic precursor and the plastic wave component (when it is present) so that both arrival times can be determined. A third type of pressure sensor that relied upon the disruption of optical fibers was carried to a late stage of development but was not actually employed in this study. Its description also appears in Section V of this report.

The results from the shock trajectory study are presented in Figure 22. Their resolution is, unfortunately, insufficient to establish the shock trajectories to the point where firm conclusions can be established.

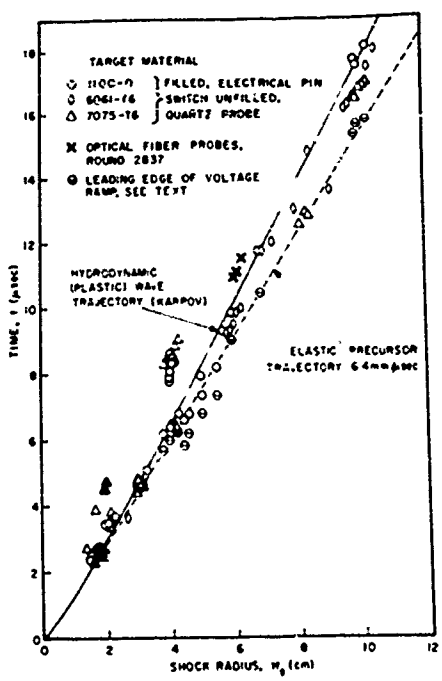

Figure 22. Shock Arrival Time vs. Depth Into Target for 1100 Aluminum Showing Dilatational (solid line) and Bulk (dashed line) Wave Velocities.

The relatively large scatter in this data has been traced to premature actuation of the impact sensor by impacts from spray particles that preceeded the pellets down range. No plans have been made to improve these measurements because better data revealing the same phenomena are available.

D. Comparison of Experimental Results With Computer Predictions

A University subcontract for performing numerical calculations covering several of the impact situations studied by Major Prater was negotiated with Shock Hydrodynamics, Inc.* They used their "STEEP" code** to model the impact situations shown in Table I. Code calculations were continued until crater growth either terminated or had progressed to the point where Shock Hydrodynamics felt that final dimensions could be predicted reliably. Peak shock pressure data was also generated as a function of depth into the target and angle measured from the axis of symmetry.

At this writing, only preliminary results from these calculations are available. They indicate that crater growth rates were predicted reasonably well but that several potentially disturbing anomalies are present. They also predict single power law relationships describing peak shock pressure as a function of distance into the target rather than the two power behavior observed. The predicted power dependence of pressure with target depth lies intermediate between the two powers observed experimentally. This qualitative deviation between experiment and theory is quite disturbing because it indicates that a significant part of the impact process has not been modeled by the code. The vast majority of the comparison work between theoretical and experimental results is yet to be done and, therefore, the conclusions discussed above should be regarded as tentatively.

---

* University of Dayton purchase order RI-49516 to Shock Hydrodynamics, Inc., 15010 Ventura Blvd., Sherman Oaks, California, Nov. 21, 1969.

**STEEP is an Eulerian visco elastic-plastic code of advanced design[12].

III. BALLISTIC IMPACT STUDIES

Recent Air Force experience in South East Asia has demonstrated that present and near-future aircraft will be subject to intense attack by small-arms fire and exploding ordnance during combat missions. Present aircraft appear to be quite vulnerable to such attack and a relatively high priority has been assigned to hardening future aircraft against these threats and. where possible, to provide "quick fixes" for current Air Force systems. These activities require relatively detailed knowledge of materials and structural response to impacts of both ogive projectiles and fragments. Velocities of interest range from below 1000 ft/sec to approximately 5000 ft/sec. Periodically, other areas of investigation require similar impacts over the velocity range described above and extending to the maximum speeds achievable with solid propellant guns. Effort in the ballistic impact area has been divided between evaluations of current and future airframe and armor equipment, and more fundamental studies aimed at determining the mechanisms controlling impact damage at ordnance velocities. Sufficient understanding of ordnance velocity impact processes is expected to yield basic design criteria for structures and armor of future aircraft that will enable them to withstand ballistic impact better than current systems.

FACILITIES

Since the initiation of Contract F33615-68-C-1138 in November 1967, two ranges have been added to the Building 44 facility(B30). One new range employs a Frankford type gun mount on a semi-universal support developed by the University of Dayton (see Figure 23a). The Frankford mount is equipped with gun tubes ranging from .223 cal. to .830 cal. Effective top velocities are near 6000 ft/sec for most projectile configurations. The older 25 mm Hotchkiss cannon system used on the original range has been made semi-portable and can be used with any of the impact setups available to the Frankford system (see Figure 23b). The Hotchkiss cannon can receive specially machined barrels ranging from .223 to .50 cal. Various other gun mounts are set up from time to time to meet special requirements and are then dismantled. Both of these guns can be pivoted to fire into any of several range areas. The largest of these is a 8' x 8' x 8' armored "house" that contains equipment for stressing targets while they are impacted. Two other range areas are available for a wide number of setups including a ballistic pendulum for measuring velocity loss during impact of thin plates and a variety of armored boxes for containing debris from impacted targets. In all cases, projectile velocities are measured before impact with make-screens ard high speed chronographs. Supplementary instrumentation systems including a fast framing camera, single frame high speed cameras, and flash x-ray generators are available for

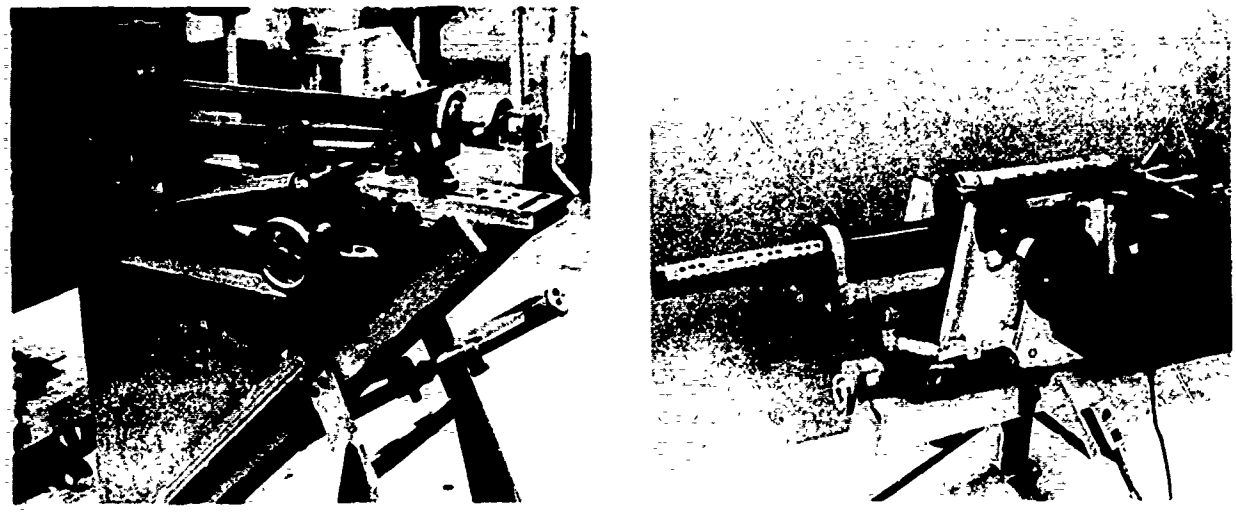

Figure 23. Frankford (a) and Hotchkiss (b) Gun Mounts.

monitoring target response to ballistic impacts and determining the characteristics of the debris generated by the impacts.

A ballistic range for more specialized studies has also been constructed in Building 56, Bay 5, at Wright-Patterson Air Force Base (see Figure 24). This range, which is built to accept guns between .223 and .830 cal., is equipped with an integral blast tank, an armored instrumentation section, and several armored target tanks. The entire trajectory from the gun muzzle to the target is armored so that special protection for nearby equipment and personnel is unnecessary. The range is equipped with a pair of high speed cameras for photographing projectiles in flight to make unambiguous determinations of their velocities and orientations relative to their flight directions. Top velocities achieved with this range have exceeded 9000 ft/sec.

Range Calibration Program

Severe divergences between ballistic limit results obtained at various facilities providing data for the Department of Defense have led to the suspicions that actual test conditions vary between facilities, and that these differences are responsible for data divergences. The Joint Interservice Body Armor Committee (JIBAC) therefore set up a series of coordinated tests designed to detect such differences and eliminate them

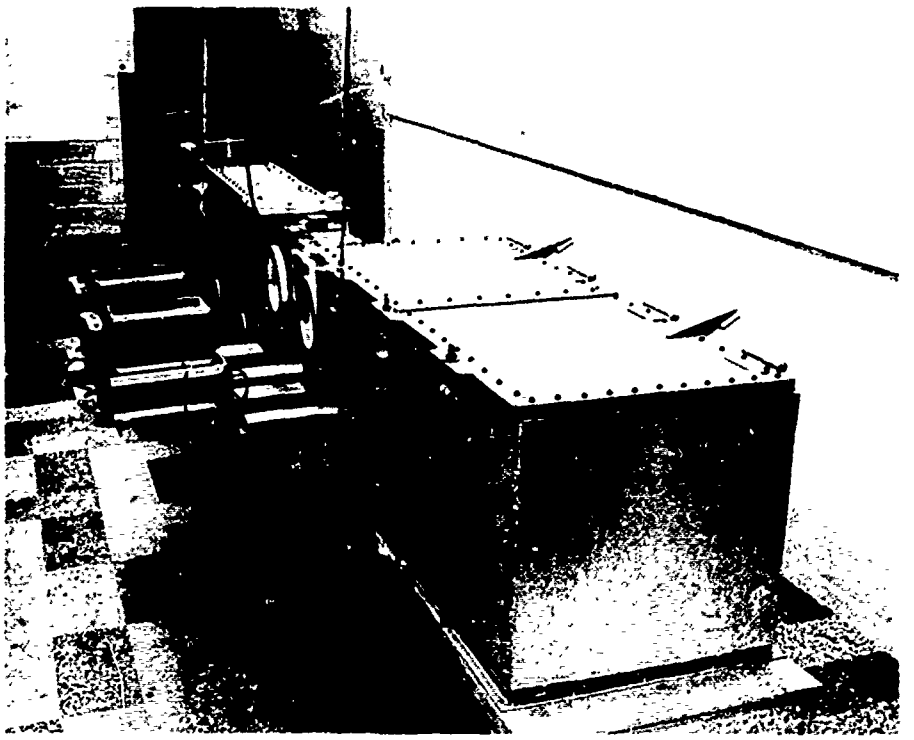

Figure 24. Armored Trajectory Ballistic Range in Building 56, Bay 5.

if they exist. The ballistic limits of several standardized impacts against selected sheets of 2024-T351 aluminum were determined at each facility. The steel projectiles consisted of 17 grain bore-launched flak simulators, 16 grain saboted 1/4" spheres, and 8 grain and 64 grain saboted cubes. The projectiles, the sabots, the guns for launching them, and the targets were supplied from a single source. The results of tests conducted by the University were reported to AFML via References B36 and B46. They indicated that rotation-stabilized flak simulators and saboted spheres could produce precisely determined (exactly reproducible) ballistic limits when fired against homogeneous targets. The cubes, which struck the targets at a variety of orientations, could not be used to generate such precise data. Other conclusions from this study were: (1) extreme care is required in measuring projectile velocities, especially when sabot launchers are employed, and velocity measuring systems using projectile photographs are mandatory if reliable results are to be obtained; and (2) cube impacts represent the most realistic simulation of fragment impacts against aircraft systems but they are too imprecise for general use when impact orientations are not controlled. The University recommends that rotational stabilization techniques be developed for launching cubes so that their impact orientations can be predetermined.

BALLISTIC IMPACT RESPONSE PROGRAM

The University conducted a wide range of fundamental impact studies involving impacts against targets representing present and future Air Force systems components. These studies were aimed primarily at elucidating impact mechanisms and establishing the effects of various types of impact damage upon component performance. The largest effort was concentrated upon the response of thin targets to impacts by small-arms ammunition. Studies ranged from response of homogeneous plates to the response of actual aircraft components fabricated from advanced materials. Other studies were concerned with performance of airborne armor systems designed to protect individual components from impact damage.

Fundamental Studies

The following section describes studies aimed to one degree or another at establishing the nature of impacts into materials used in current or near-future aircraft. Whenever possible, studies were structured to produce data directly applicable to specific Air Force problems.

Ballistic Response of Single Sheets

A vast majority of airframe components that are struck by small-arms fire and shrapnel are structures containing flat plates. These plates which make up most of the outer skin are load bearing and hence strength degradations caused by ballistic impacts are of prime importance to establishing aircraft combat vulnerability. Earlier, a detailed analysis of aluminum honeycomb panels used in the F-111 airframe was carried out[18]. Results from this study indicated that impacts from small-arms ammunition, particularly at high angles of obliquity, can have an effect upon the strength of honeycomb panels. The F-111 study left a number of questions unanswered concerning the effects of chemically milling the honeycomb skin, and the effects of sharp cracks in the skins at the edges of impact damage. Studies were carried out during the current effort to resolve these questions and to provide other fundamental data about the response of thin metallic plates to ballistic impacts.

The chemical milling process may change the impact response of plates due to selective removal of alloyed elements near the exposed surface. Possible effects upon ballistic response of such plates were investigated by comparing the residual strength after impact of chemically milled sheets with that of otherwise identical sheets of rolled aluminum[B41]. The sheets were impacted by .30 and .50 cal. projectiles and were subsequently stressed to fracture. No significant differences were observed between damage and residual strengths after impact with the possible exception that, occasionally, chemically milled sheets generated slightly longer cracks adjacent to the impact sight.

Theoretical fracture mechanics indicates that, under certain circumstances, sharp cracks will propagate across stressed plates causing catastrophic failures while disturbances with rounded edges will not permit such cracks to start. Should the 2024-T86, 2024-T81, and 2024-T62 chemically milled plates be in the proper metallurgical condition, slight differences in cracks generated by impacts in unstressed plates, could strongly effect overall residual strength. This possibility was investigated by comparing the tensile strengths of impacted plates with those of similar plates that had holes drilled in them the same diameter as the longest crack span(B52). No significant differences between the residual strength of impacted and drilled plates were observed; this result indicated that the fracture toughness of the plates was high enough that the residual strength of plates after impact can be treated by simply accounting for the overall span of the resultant cracks.

Early investigations at this facility have indicated that projectile energy absorption during impacts with airframe structures is one of the most crucial parameters determining both the modes and extent of structural damage. Minimum damage appears to occur when impacting projectiles perforate the structure with a minimum loss of kinetic energy. A number of analytical theories are available for predicting the energy lost during impact of various projectile shapes including spheres, flat cylinders, ogives, etc. A program was initiated to evaluate several conflicting theories describing such energy losses with experimentally obtained data*. A ballistic pendulum (described in the instrumentation section of this report) was used to measure velocity losses of a variety of projectile shapes as they perforated 6061-T6 aluminum and cold rolled steel targets. All shots were carried out at a single velocity of 0.52 km/sec but a variety of target thicknesses were investigated. Major Fields was able to demonstrate that one of the theories (due to Nishiwaki)(19) is probably adequate for evaluating projectile energy loss from impacts normal to the target surface.

The extreme strength and rigidity provided by advanced composite plates has created strong interest in their use as skins of honeycomb panels for future aircraft components. These materials have been developed to the point where experimental control surface panels made from boron-epoxy-honeycomb have been fabricated and tested on F-111 aircraft. The ballistic response of such panels will be a determining factor in the combat vulnerability of future aircraft should wide use be made of this technology. The University examined the response of composite sheets made from boron fibers in an epoxy matrix and found that their ultimate strengths

* This program was carried out with the support and guidance of the University by Maj. T. E. Fields as his Air Force Institute of Technology Master's Thesis (see Ref. B28).

were reduced by impacts to a significantly greater extent than sheets of more conventional honeycomb skin materials[B42, B47]. The most widely believed hypothesis for explaining these extreme strength reductions in the boron composites is that the load sustained by the boron fibers initially broken by the impact is transferred almost entirely to the fibers immediately adjacent to the impact which then fail in tension thus loading their adjacent fibers. This phenomenon continues until catastrophic failure occurs. A question immediately arises as to whether this phenomenon is related to the extreme absolute rigidity of boron fibers or simply to the enormous ratio between the rigidities of the fiber and epoxy. Tests were set up to investigate this question by comparing the boron panel strength reductions with those of similar fiberglass panels (the rigidity of the glass fibers is large with respect to the epoxy matrix material but is small with respect to the boron)[B45]. Unfortunately, the fiberglass panels chosen for the initial study were designed for another purpose and their loading surfaces could not be made strong enough at the mounting fixtures to withstand stresses required to fail them in the region of the impacts. Other studies with properly-designed fiberglass panels are planned for the future.

Response of Honeycomb Structures

Experimental sequences closely following the ones described above for plates have been conducted with honeycomb panels that are either in actual use today or are planned for use with airframes now under development. Results from these tests are notably similar to those for the single plate tests and, in all cases, substantiate the predictions made on the basis of single plate tests[B40, B55].

Ceramic Armor Investigations

Armor systems utilizing ceramic tiles as their principal elements have significantly reduced the weight requirements for aircraft protection from ballistic penetration. Past theoretical and experimental studies have disclosed that, during the impact of a projectile or fragment simulator, several impact processes are at work to destroy the target and projectile. Wilkens[20] has carried out detailed investigations of the mechanisms controlling ceramic armor operation which demonstrate that the resisting forces of both the intact ceramic and properly-supported powdered ceramic are responsible for fracturing the metallic cores of impacting AP rounds. The resulting impulse from the ceramic and projectile debris is spread over relatively large areas of properly-designed backup structures, thus leading to large overall reductions of impulse intensities felt by the substrate. These factors allow significant reductions in the areal densities of backup structures without concomitant reductions in ballistic protection.

An effort was initiated to investigate the ballistic response of ceramic armor with a fiberglass backing material*. The effort was to

study the operating characteristics of ceramic armor, to determine conditions under which the armor is most effective, and to point the way toward future concept development. The effects of several parameters such as tile size, thickness, substrate characteristics and substrate support upon V_{50} determinations were established. Dynamic measurements of the impact process were carried out, which included taking shock measurements and sequenced flash radiographs of the impacts plus using dynamic photographs to make rear-surface measurements behind the ceramic tile and the backup structure. The data from these studies will be compared with similar measurements and predictions from Wilkens' work in order to evaluate the effects of AP jackets and liner materials upon perpendicular impacts into ceramic armor panels.

Engineering Data Tests

Primary emphasis of the efforts described below was to obtain data applicable to specific Air Force problems needing immediate attention. Whenever possible, the experiments were adjusted to provide data of more general interest as well as that needed for the problem at hand.

Losses of tactical and strategic aircraft to antiaircraft and small-arms fire are a matter of serious concern. The loss rates of present military aircraft in the current conflict should be reduced significantly by installing additional armor to increase protection of operating personnel and selected critical components.

The University is conducting ballistic evaluations of dual-hardness steel for use as aircraft armor. (supplied GFE)(B50, B57) The armor is made much harder on the impact side than on the exit side. The purpose of the hard surface is to fracture the metallic cores of impacting AP rounds and to spread the projectile debris over a relatively large area; then it is absorbed by deformation of the relatively soft backup material. The results of the armor material tests are expressed in terms of the velocities required to achieve V_{50} ballistic limits with standard AP ammunition. This ballistic limit is defined as the conditions required to generate a 50% probability that material and debris ejected behind an impacted panel will perforate a 0.020" thick sheet of 2024-T3 rolled aluminum spaced one foot behind the target.

In addition to ballistic protection, personnel and cargo in large transport aircraft must be protected from noise and heat. The University initiated a study to obtain thermal, acoustic, and areal density measurements of seven candidate blanket-type materials for use as fragment,

---

* This effort was carried out with the support and guidance of the University by Capt. J. Teal as his Air Force Institute of Technology Master's Thesis, "(U)The Effect of Tile Size and Mounting Procedure on the Ballistic Limit of Ceramic Composite Armor", Confidential Report, GAW/MC/70-6.

noise, and heat shields against the inside skin of air transports[B59]. The best material tested (on the basis of thermal and acoustic merits of single-layers of the materials) was a non-woven fiberglass insulating felt incased in a plastic sheet. The second best material was a thick white felt known to have a good ballistic protection value.

Component Tests

Air Force experiences in South East Asia have demonstrated that helicopters are subject to intense attack by small arms fire and exploding ordnance during combat missions. The University conducted a study to determine the vulnerability of a stressed Model 209AH-1G helicopter blade to .50 cal. impacts. The blade was loaded in bending and impacted at 25%, 50%, 75% and 100% maximum design stress levels. The various design stress level impacts showed little difference in the damage generated. An attempt was made to fail the blade by firing a number of impacts in one area with the blade being stressed above its designed levels; however, the blade prevailed. A number of .830 cal. impacts are planned in the near future.

The F-111 windshield and canopy is also subject to intense attack by small arms fire and exploding ordnance during combat missions. The University conducted a study to determine the damage and penetration effects from .30 cal. impacts into the panels at various angles of obliquity. Two types of glass were evaluated at various angles of obliquity and projectile velocities.

The University also conducted a study to determine the ballistic limit of a B5-MA1 parachute back pack[B44]. Such packs may provide ballistic protection to aircraft personnel if they are worn during missions in combat areas. The parachute was impacted with .22 and .30 cal. fragment simulators. Results indicated that the back packs provide significant protection to the wearer but sustained relatively serious damage that could easily make them unusable for their primary function. Thus, the question is opened about whether the back packs should be protected as well as the aircrew member.

IV. ONE-DIMENSIONAL IMPACT PROGRAM

Planar shock waves have been used for many years for studying dynamic response of materials subjected to extremely high pressures[21, 22]. The very simple geometrical considerations of planar shock wave analyses allow them to be carried out with fewer computational difficulties than any other geometrical arrangement. Four parameters fully describe materials state behind propagating shock waves:[23] (1) material internal energy, (2) material velocity (particle velocity), (3) shock wave velocity, and (4) shock wave stress (or pressure). Three fundamental conservation relationships known as the Hugoniot jump conditions may be employed to describe uniquely all of the materials state variables if any pair of them can be determined independently. The strategy of materials investigations employing one-dimensional impacts is to measure some pair of these relationships for a particular shock wave situation so that all four of the shock parameters may be evaluated. Such measurements carried out upon samples of a particular material subjected to a range of shock amplitudes can be used to derive a shock adiabat (Hugoniot) for the material. Hugoniots have been established for several hundred materials including homogeneous metals, plastics, composites, and minerals[24]. These data have proved to be extremely valuable for predicting the response of materials to environments capable of generating shock waves (not necessarily planar ones).

Planar shock waves have been produced by a number of techniques in the past but they fall into two general categories. The first relies upon the material sample being in contact with an explosive charge which is detonated to produce a planar explosion front parallel to the sample interface that propagates toward it[25]. The second and more widely used group of techniques relies upon impacting the sample with a flat plate of homogenous material to produce a planar shock wave. Peak shock pressures can be varied over extremely wide ranges by controlling the shock properties of the impacting plate and the impact velocity. A particular class of impact experiments are those where the impacting plate is extremely thin so that the duration of the shock wave generated in the sample is extremely short (plate slap experiments)[26]. These experiments have been employed widely to simulate various effects arising from nuclear attacks upon space vehicles.

The University of Dayton has operated a plate slap facility whose main purpose has been the screening of present and candidate RV materials with respect to their abilities to withstand short-duration shock loading[B31]. More recently the development of a powder gun impact facility has been initiated. This facility, of radical new design, has the potential for

opening new areas of shock pressure and measurement precision that cannot be achieved with any current facilities.

THE ELECTRIC PLATE SLAP FACILITY

Basically, the plate slap facility uses the plasma generated by exploding a metallic foil with an electrical pulse to accelerate a thin Mylar sheet (flyer)[27]. Power for the foil explosion is provided by a bank of energy storage capacitors. After the acceleration, the flyer's velocity is measured photographically and the flyer is allowed to impact the material under study. The planar impact of the flyer with the target sample causes a shock wave to propagate forward into the sample and rearward into the flyer. The rearward traveling compression wave in the flyer reflects in tension at the rear of the flyer and recrosses the flyer to the target interface where it starts destressing the original compression wave in the sample[28]. Shock pressure (a function of impact velocity) and shock duration (a function of flyer thickness) can be chosen independently to simulate nuclear weapons effects upon material samples.

High Voltage Bank

A 100 kV, 15 kilojoule capacitor bank constructed earlier was "shaken down" during the present contract effort[B27]. It is capable of launching flyers at atmospheric pressures to velocities between 1.0 and 3.0 mm/μsec[B31]. The low inductance, high voltage geometry chosen for this capacitor bank yields good flyer planarity (temporal planarity averages between 0.5 and 1.0 μsec) and velocity reproducibility. A record of flyer velocity versus bank-charging voltage is presented in Figure 25. The electrical parameters of the capacitor bank were measured using di/dt probes[29] and are presented in Table II.

Table II

Capacitor Bank Electrical Characteristics

	High Voltage Bank	Low Voltage Bank
Maximum Voltage	100 kV	20 kV
Capacitance	3 μf	56 μf
Inductance	104 nh	132 nh
Load Resistance	51 mΩ	31 mΩ
No Load Resistance	21 mΩ	10 mΩ
Critical Damping Resistance	372 mΩ	97 mΩ
Ringing Frequency	280 kc	58 kc
Current Reversal	54 %	23 %
Peak Current	4.1 amp/volt	14 amp/volt

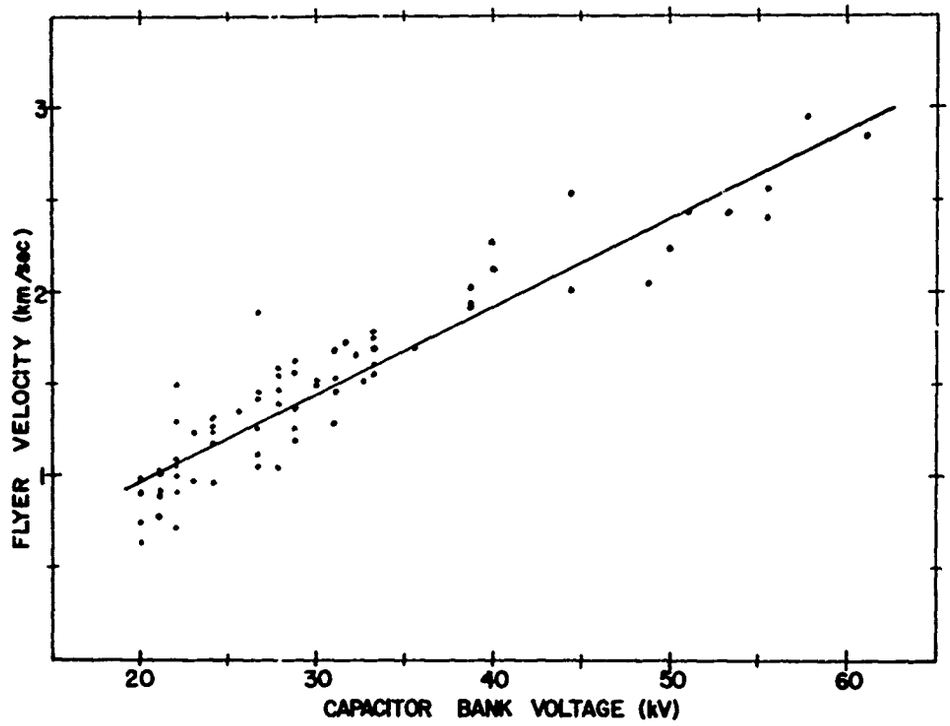

Figure 25. Flyer Velocity vs. Charging Voltage of the High Voltage Bank.

Low Voltage Bank

Air trapped between a target and an impacting flyer has been observed to lower the peak shock pressure achieved in the target and lengthen the pressure pulse duration[30]. An obvious solution is to evacuate the flyer trajectory. This solution cannot be carried out easily because the dielectric strength of a readily achievable vacuum (10^{-3} to 10^{-1} torr) is so low that it would permit electrical breakdown around the plasma channel[31]. A widely employed solution is to produce a hard vacuum in the trajectory--a cumbersome and lengthy procedure. Another facility has achieved noteworthy success in avoiding the breakdown problem and high vacuums by using a lower voltage capacitor bank*.

A low voltage, high capacitance system was decided upon for a new facility to launch flyers in a vacuum. The capacitor bank was constructed to accommodate a small, expendable vacuum chamber which could be quickly pumped down to 5 - 80 x 10^{-3} torr with a small mechanical forepump. Four 20 kV, 14 μf capacitors interconnected with a parallel-plate transmission line are used to provide the required energy pulse. The

* Dr. D. V. Keller of Effects Technology, Inc., Santa Barbara, Calif. has been successful with a 20 kV, 56 μf capacitor bank for vacuum work.

exploding foil transducer is clamped between an isolated section of the transmission line and a one-inch thick aluminum ground plate. The isolated section of the transmission line is switched to the collector plate which is directly connected to the capacitors with a triggered spark gap. Figure 26 shows the low voltage capacitor bank with the B&W 300 framing camera and the high voltage capacitor bank in the background. The electrical characteristics of the low-voltage bank are listed in Table II. The low voltage facility can launch 3.8 cm square by 0.127 mm thick (1.5 x 1.5 x 0.005 in.) flyers at any velocity between 1.0 and 3.0 km/sec.

A vacuum transducer (shown in Figure 27) has been developed which is extremely simple to construct. This transducer remains separated into its two constituent pieces, the exploding foil assembly and the 7 cm high vacuum chamber, until it is prepared for firing[B31].

The low voltage transducer for operation under normal atmospheric conditions is essentially a copy of the vacuum transducer--the only difference being that a short Plexiglas barrel is mounted on the exploding foil assembly in place of the vacuum chamber.

Two principles have long been used for the design of high voltage plate slap systems: (1) the magnetic driving force produced by a close backstrap geometry should be used to supplement the pressure exerted by the expanding plasma; and (2) the capacitor bank's inductance should be minimized in order to maximize the rate of energy deposition in the resistive arc channel. It soon became obvious that one or both of these principles might not apply to low voltage discharge systems operating in "soft" vacuums. A prolonged shakedown time was encountered in the low voltage bank development. The reproducibility of the flyer velocities and the production of sufficient quality photographs were severe problems during this period. It was decided to eliminate the backstrap geometry altogether. An electrode was extended out to form a rectangular horizontal loop from one side of the top of the parallel plate transmission line to the other side as shown in Figure 28. The transducer was placed inside the loop and electrically connected to the loop on one side of the transducer and to the ground plate of the bank on the other. This transmission line geometry nearly tripled the inductance of the system but led to noticeably higher reproducibility and higher quality photographs of the flyer in flight. The resultant shape changes in the magnetic field associated with the discharge pulse may have a stabilizing effect on the plasma beneath the flyer since the currents flowing to the transducer on either side of it are in the opposite direction to the current passing through the transducer to the ground plate. Such a situation produces a net repulsion of the current carriers which impedes lateral expansion of the discharge plasma. The final improvement was made when a section of the support directly beneath the transducer was removed. This left the bottom of the transducer a free surface which changed its shock reflection characteristics such that a

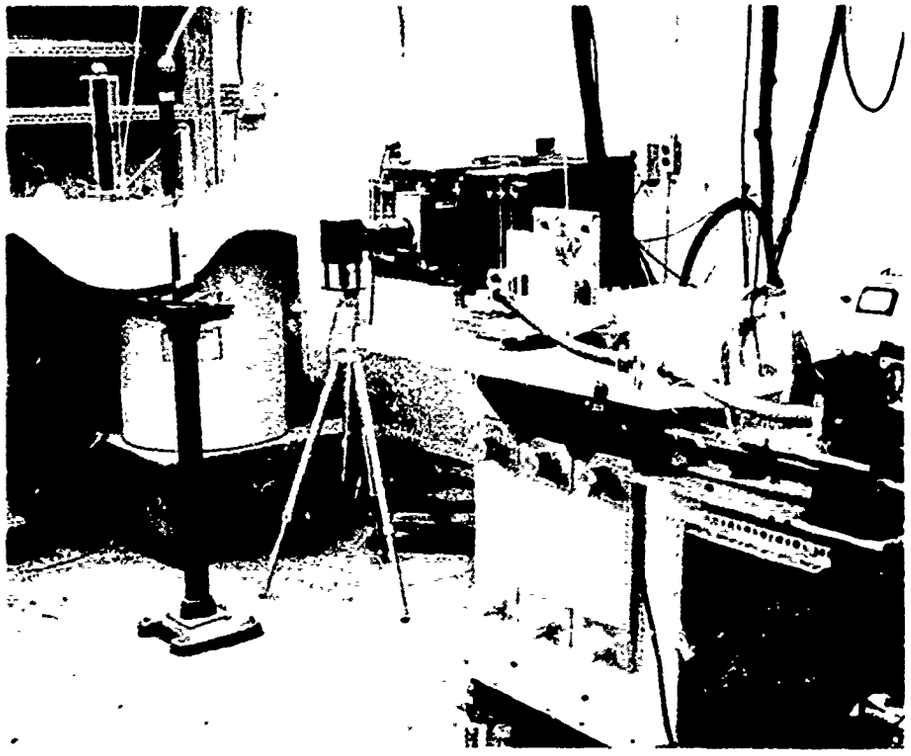

Figure 26. Low Voltage Bank With the B&W 300 Camera and High Voltage Bank in the Background.

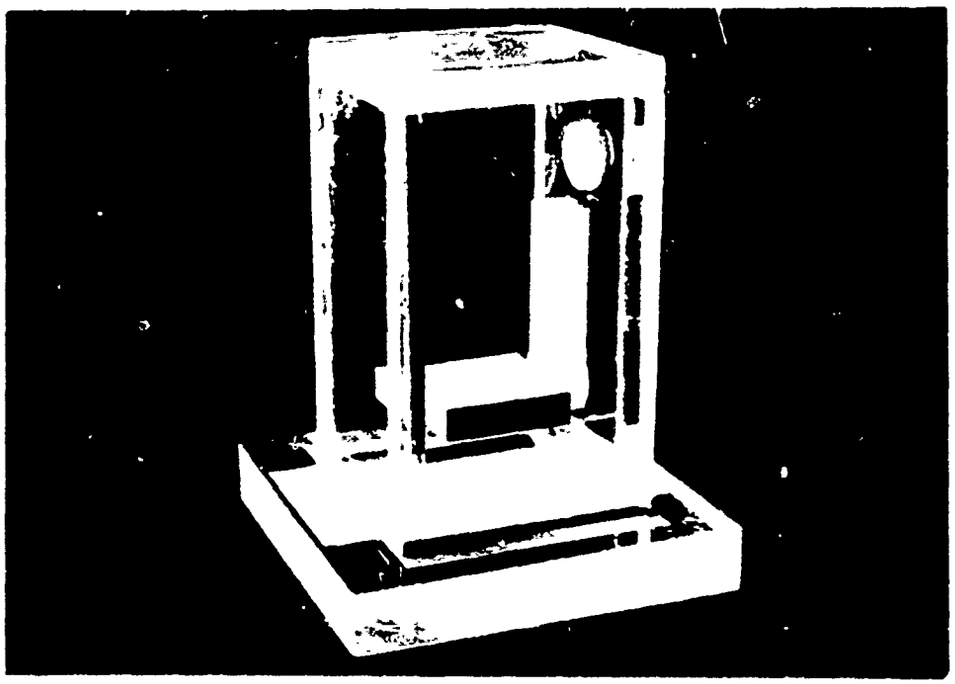

Figure 27. Low Voltage Bank Vacuum Transducer.

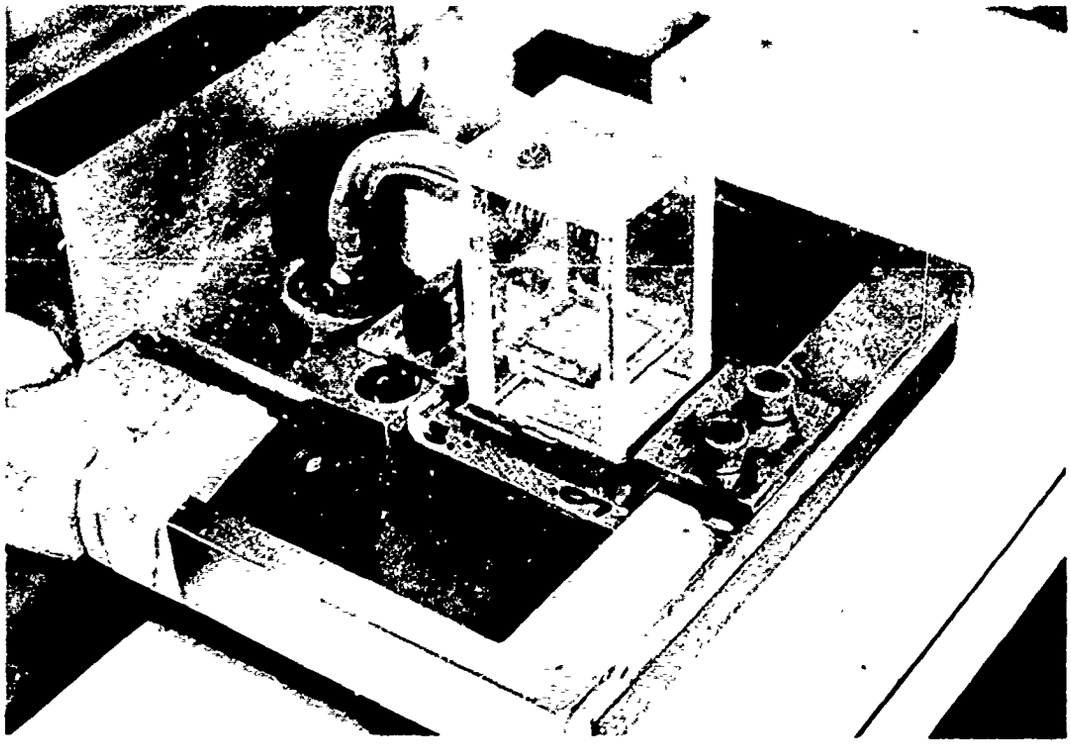

Figure 28. Vacuum Transducer in Place on Low Voltage Bank.

release wave from this free surface could interact with the expanding plasma.

Figure 29 is a plot of flyer velocity versus bank voltage for the low voltage bank when used to launch 3.8 x 3.8 x 0.0127 cm flyers. The lines radiating from the origin represent constant efficiencies as labeled. The plot indicates that the system efficiency has a maximum (19%) when charged to approximately 8.5 kV.

RIFLE Transducer

Great difficulty in launching flyers with velocities between 0.4 and 0.8 km/sec has been encountered both at this facility and elsewhere. The low energy deposition required to produce a flyer velocity below 0.8 km/sec is insufficient to explode the foil uniformly. As a result, non-simultaneity of impact and spacial impulse gradients render the standard transducer unreliable at velocities below 0.8 km/sec. The shock transfer block transducer which relies upon shock waves in a solid block to launch a flyer affixed to the free surface functions well until the flyer velocity reaches approximately 0.4 km/sec. The block itself fails via spallation if a higher flyer velocity is attempted; and the spall layer, along with the flyer strikes the target, thereby compromising the results.

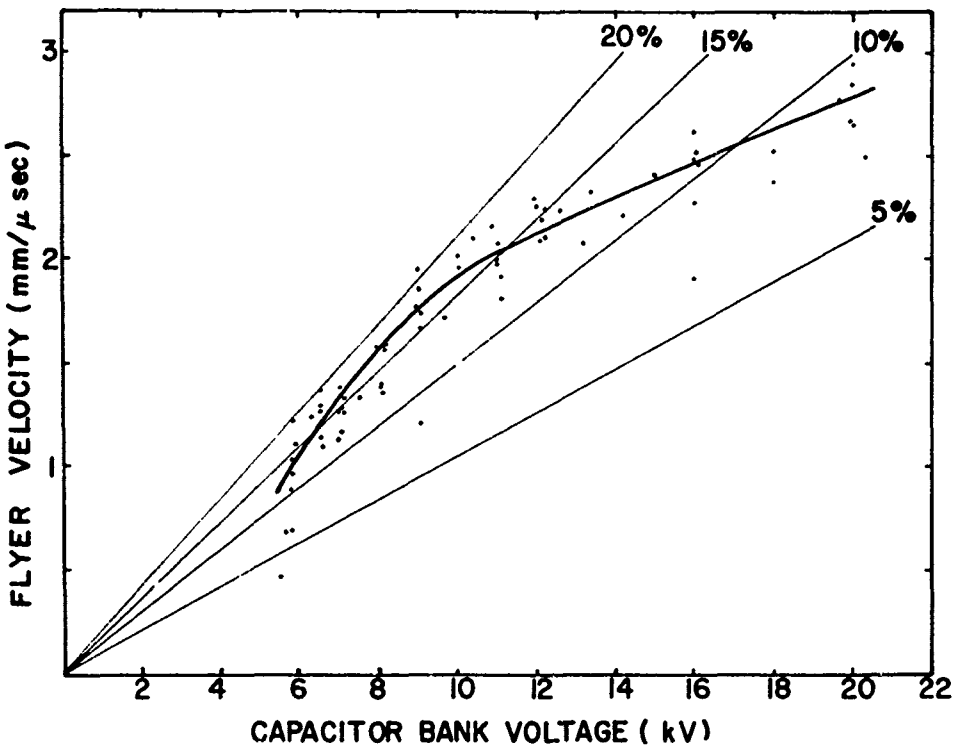

Figure 29. Flyer Velocity vs. Bank Charging Voltage for the Vacuum Transducer.

A high voltage transducer with a velocity capability of between 0.4 and 0.8 km/sec has been developed recently as a modification of the standard transducer[B5]. A peak pressure of between 10 and 20 kilobars is produced in the plasma of the standard transducers very shortly after the electrical explosion of the foil since the initial plasma density is essentially that of the solid foil*. To reduce this pressure and the resulting flyer acceleration, an open gap is built directly beneath the foil as shown in Figure 30. This breech cavity of between 6.4 and 13 mm in depth allows the plasma to free-expand downward thus significantly reducing the impulse available for launching the flyer upward. This launching device has been named RIFLE (Reduced Impulse Flyer Launch Element).

In the standard launching device, flyer velocity is a function only of the energy deposited in the foil before and during flyer launch. However, in the RIFLE geometry, flyer velocity can be varied by changing either the energy deposited in the foil or by changing the breech depth. Two depths have been investigated and the larger volume breech yielded lower velocity flyers than the smaller volume breech when all other parameters were held constant.

---

* This pressure was calculated using a computerized mathematical model of the exploding foil launch process developed by one of the authors (P. W. Dueweke). This model and the results thereof will be reported in a later section.

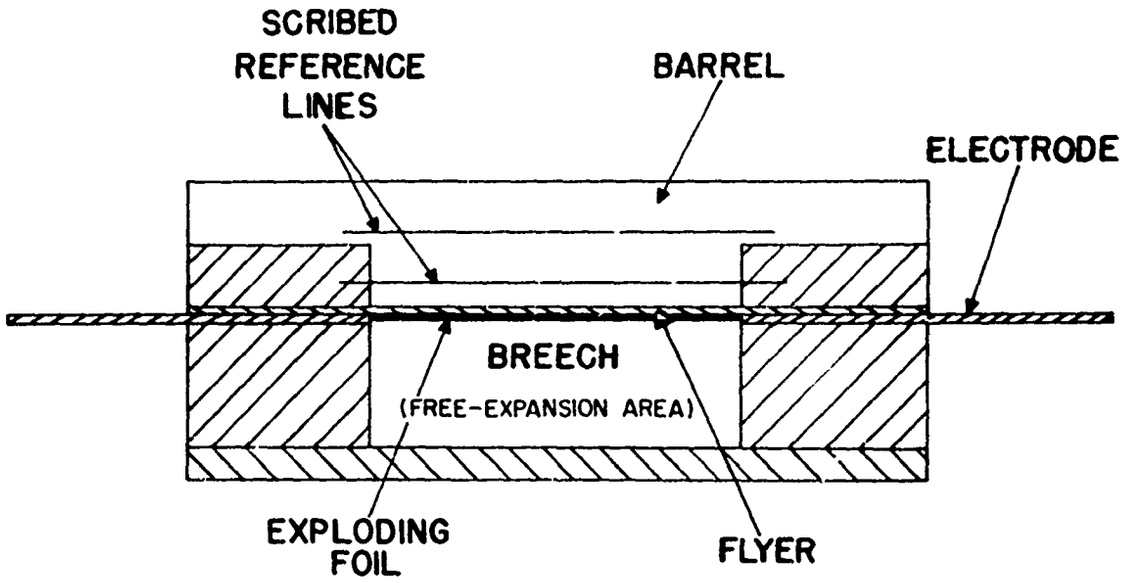

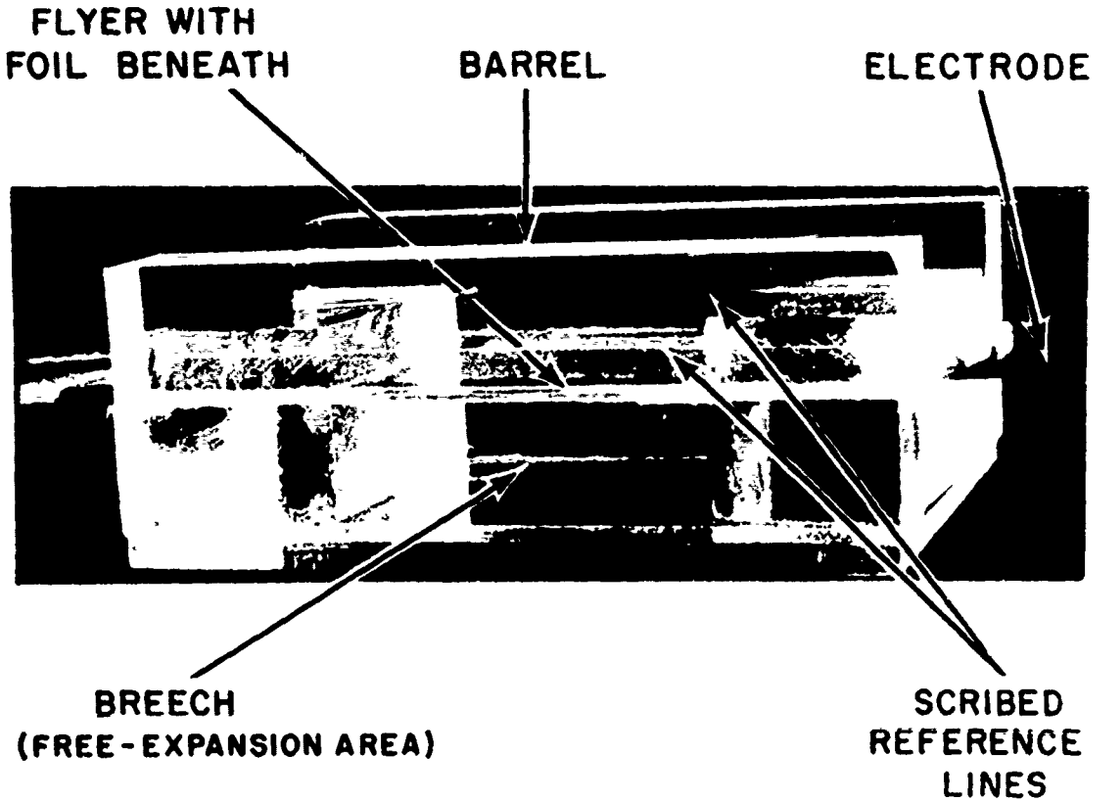

Figure 30. Intermediate Velocity Transducer (RIFLT).

Figure 31 shows the velocity-voltage calibration curves for the 13 mm and the 6.5 mm RIFLE. Each set of data was fitted to a least squares line. The standard transducer calibration curve is also shown. A median spacial planarity of 0.4 mm has been measured for all RIFLE shots with more than one-quarter of the planarities less than 0.2 mm when precautions were taken to insure that the plasma pressure was much greater than that needed to shear out the flyer. This condition can be met by partially precutting the flyer around the inside edge of the barrel where it is to shear upon explosion of the foil.

Fly-Off Plate Measurements

The rear (free) surface of a solid moves under the stress of a compression wave at approximately twice the material particle velocity. Plates attached to the free surface with a zero tensile strength bond will be launched at the same velocity at which the surface moves[32]. A capability to measure the velocities of fly-off plates affixed to target rear surfaces has been developed. The fly-off plates were made from a number of materials--from 1/16" Plexiglas to 2 mil aluminum--and were attached to the target rear surface with vacuum grease. A medium speed framing camera (B&W Dynafax Model 326B) was used to monitor fly-off plate motion during plate-slap experiments. Altogether ten fly-off plate velocities were measured. The fly-off plate velocities and flyer velocities ranged from 0.03 and 0.48 km/sec to 0.30 and 1.31 km/sec, respectively.

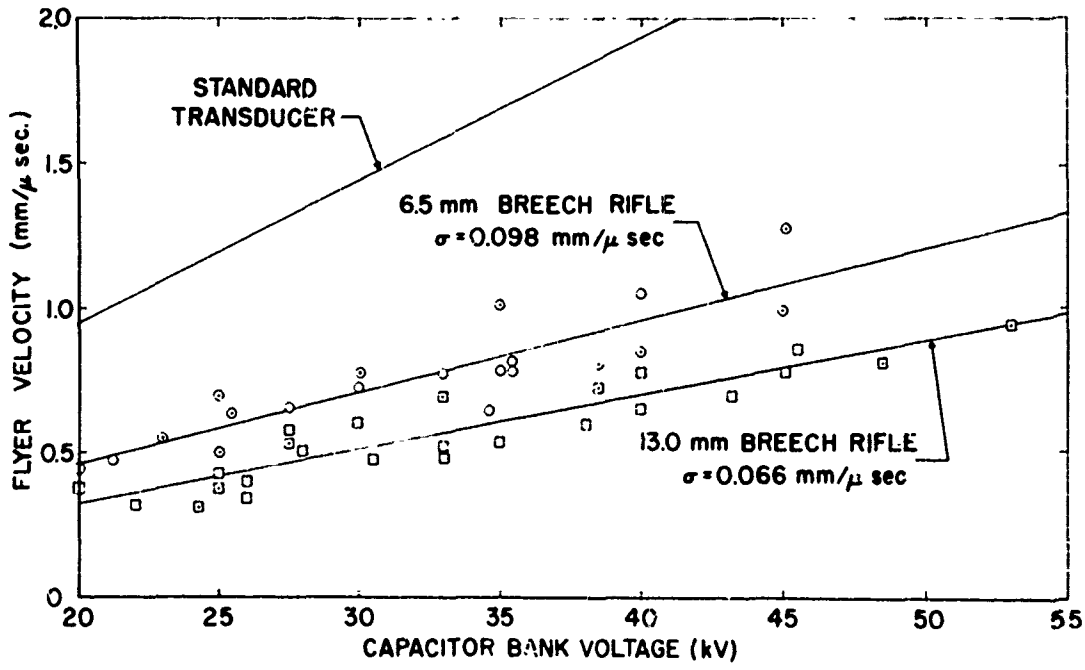

Figure 31. Flyer Velocity vs. Bank Charging Voltage for the RIFLE Transducers.

Theoretical Model of the Flyer Launch Process

The flyer velocity and acceleration profiles have been calculated theoretically from a combined thermodynamic-mechanical analysis of the plasma column expansion. The physical model is based on the rate of energy deposition into a classical macroscopic system. Experimentally determined capacitor bank electrical parameters were used to determine the current through the foil[29, 33]. This current was then translated into Ohmic heating to explode the foil. The resistance was determined from the damping rate of the bank discharge current.

A computer program was written to increment time in 5 nsec steps while calculating each of the variables for each step. The analysis considers the following processes:[34] (1) the foil heats uniformly at constant volume to its melting point; (2) it melts at constant temperature and volume; (3) the molten foil heats uniformly at constant volume to its boiling point; (4) the foil vaporizes at constant temperature and volume; and (5) the aluminum vapor expands isentropically as an ideal gas shearing the flyer and accelerating it ahead of the expanding cloud. During this last process the gas is assumed to radiate as a black body.

The analysis was carried out for typical situations set up for both the high voltage bank (HVB) and the low voltage bank (LVB). Figure 32 presents selected results from both analyses. It has been determined empirically that the flyer acceleration is insignificant after approximately 0.3 cm of flight[B27]. Thus the theoretical curves in Figure 32 express the velocity achieved at this point in the launch. The physical model applied to the HVB differs from that applied to the LVB only in that the former employs the magnetic backstrap effect to help accelerate the flyer whereas this phenomenon is non-existent in the LVB discharge geometry.

The peak plasma pressures produced by the LVB at 20 kV and by the HVB at 60 kV are 14.5 kbar and 25.1 kbar respectively; however, high pressure is maintained for a longer time on the LVB than on the HVB. The peak temperatures for the LVB and the HVB are 50.8×10^3 °K and 54.1×10^3 °K respectively.

At least three additional phenomena have been added to the model to determine their effects upon final flyer velocities. First, a power series equation of state for the plasma was used to replace the ideal gas law. The compression of the backup plate beneath the exploding foil was evaluated under the load of the high pressure plasma. Finally, the internal energy of the gas was partitioned among the atoms and a hard-sphere atomic model was calculated using a Lennard-Jones interatomic potential. This volume was then subtracted from the macroscopic plasma volume to find the volume available for atomic motion. None of these schemes yielded any significant differences in the final results.

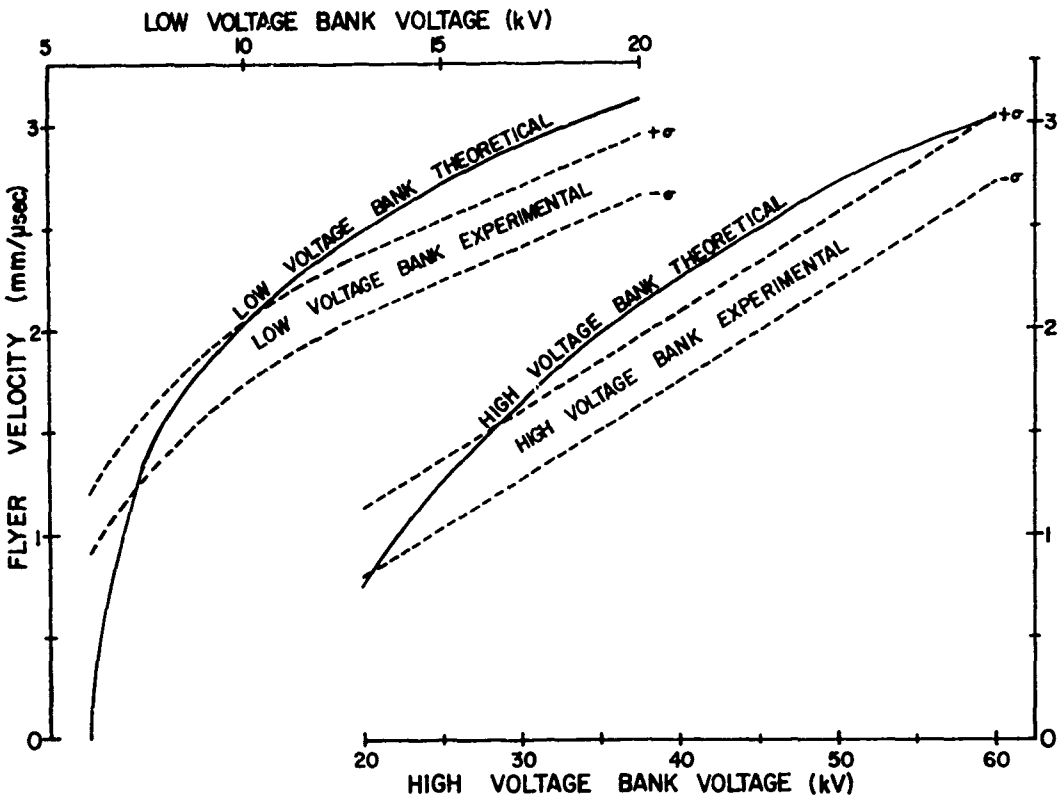

Figure 32. Comparison of Flyer Velocity Determined by Theoretical Analysis and by Experiments.

Flyer and Shock Wave Planarity Considerations

The typical data analysis exercise includes considerations of such factors as flyer velocity, flyer planarity, and the velocity gradient over the flyer surface due to non-planarity.

The assumption is made that all points on the flyer are launched at the same instant (i.e., all parts of the foil explode at the same time), and that any non-planarity at a later time is due to velocity gradients across the surface of the flyer. This velocity variation is[B31]

$$\Delta V = V\left[\frac{\Delta s}{2s - \Delta s}\right]$$

where V and Δs are the measured flyer velocity and spacial planarity respectively, and s is the distance from the flyer's initial position to the impact plane.

A minimum allowable planarity can be calculated which will just prevent a dilatational wave generated at one impact point from interfering with the shock wave generated at a later impact point. By setting the flyer closure velocity equal to the material sound speed, this maximum

allowable impact time duration, τ, was found to be[B31] $\tau = 1.0$ μsec for a 2.5 cm square aluminum target assuming the average geometry shown in Figure 33.

The rear surface breakout velocity, i.e., the closure velocity of the shock wave with the target's rear surface, is equal to the closure velocity of the flyer-target interface[B31]. The angle, ϕ, between the rear surface and the shock front, however, will be significantly larger than the angle, θ, between the flyer and the target when the flyer velocity, V, is less than the shock velocity, D. These angles can be calculated from

$$\theta = \text{Arctan} \frac{V\tau}{x}$$

$$\phi = \text{Arctan} \frac{p\tau}{U\rho_o x}$$

where p, U, and ρ_o are the Hugoniot pressure, particle velocity, and unshocked material density, respectively. These equations were used to determine the dependencies of θ and ϕ on flyer planarity for various flyer velocities for the impact of a Mylar flyer on an aluminum target. Again, the "average" impact geometry of Figure 33 is assumed. It should be noted that despite the amplified angle of the shock front, its temporal

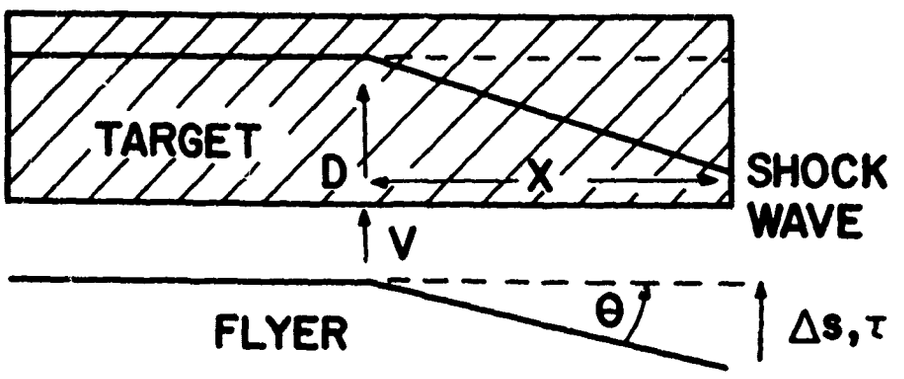

Figure 33. Average Flyer Impact Geometry.

planarity is identical to that of the flyer; and the particle velocity vector behind the wave front is directed normal to the target surface, i.e., parallel to the flyer velocity vector. Thus the same criterion determined in the flyer planarity analysis can be applied to the shock wave planarity at the rear surface.

DAMAGE THRESHOLD STUDIES

All targets impacted with the high voltage facility were mounted in such a way that they were acoustically isolated from the transducer except for air disturbances. The isolation mechanism consisted of suspending the target atop Mylar leaves extending from the top of the transducer barrel at each of the four corners. The edges of ceramic samples were wrapped with fiber tape to inhibit scattering of large fractured pieces. Their rear surfaces were color coded so that the targets could be more easily reconstructed in case of breakup. All the targets that were tested under vacuum were impacted on the low voltage bank under vacuums ranging from 5 to 80×10^{-3} torr and were acoustically isolated from the transducers. This isolation mechanism consisted of attaching the target to the vacuum chamber walls with heavy bonds of a low shock impedance rubber adhesive. Two different target edge support techniques were used for the vacuum firings--steel shock block supports and free surface supports. The steel shock block supports are 6.3 mm x 6.3 mm x 31 mm steel blocks mounted in intimate contact with the target edges (thin vacuum grease interface) and held in place by winding with fiber tape. The shock block-target package is acoustically isolated from the transducer with the rubber adhesive bonds. The free surface technique involves mounting the targets without edge supports. Table III presents the material studied along with their experimentally-determined damage thresholds.

POWDER GUN ONE-DIMENSIONAL IMPACT EXPERIMENTS

A program was initiated to study the shock response of material samples by impacting them with flat plates launched by solid propellant (powder) guns.* The guns used for this study are capable of launching flat plates to a maximum velocity of 2.5 km/sec. A two-stage gun (light-gas gun) also available for these studies is capable of velocities in excess of 8.0 km/sec. Powder guns with 40 mm bores and light-gas guns with 20 mm bores have been used for similar experiments at other facilities; however, the targets are mounted more than 1.5 m from the gun muzzles. Impact planarity attainable in such facilities suffers somewhat because of the extended free-flight path (impact angles of 0.5° are typical). These

*This initial study was carried out with the support and guidance of the University by Mr. A. K. Hopkins as his Air Force Institute of Technology Master's Thesis (GAW/MC/70-4), AFML-TR-70-158, May 1970.

Table III

Damage Thresholds for Selected Materials

Material	Thickness (mm)	Support	Damage (Taps)	Threshold km/sec	Sonic Velocity km/sec
		High Voltage Capacitor Bank			
6061-T6 Al	3.18	free surface	2050	1.18	
Teflon (UD supplied)	6.35	free surface	2200	1.3	
Teflon (AF supplied)	3.18	free surface	1300	0.75	
Teflon (AF supplied)	6.35	free surface	1300	0.75	
Teflon (AF supplied)	9.52	free surface	1400	0.80	
Slip Cast Fused Silica	9.52	free surface	750	0.43	
Feracine	6.35	free surface	<1100	0.63	
Boron Nitride	12.70	free surface	>5100	2.9	
Boron Nitride	6.35	free surface	7000	1.6*	
		Low Voltage Capacitor Bank			
Boron Nitride**	6.35	shock blocks	>5200	3.0	
7075-T0 Al	6.35	free surface	2300	1.3	6.1
7075-T0 Al	6.35	shock blocks	2100	1.2	
7075-T6 Al	6.35	free surface	2400	1.4	6.1
7075-T6 Al	6.35	shock blocks	2200	1.3	
2024-I***	6.35	free surface	2200	1.3	6.4
2024-II***	6.35	free surface	1900	1.1	6.4
2024-III***	6.35	free surface	2000	1.1	6.4
TRIP Steel	2.54	free surface	500-1700	0.29-1.0	5.7

* A 10 mil flyer was launched in this case; the others are 5 mil flyers.

** Series included 10 different porosities and additive concentrations.

*** Each of these represents a slightly different heat treating.

guns have smaller bores than their predecessors--the more common cold-gas-guns that have been used to generate most of the precise shock response data available today. Selected instrumentation techniques developed for cold-gas-guns were scaled down in size to accommodate the reduced impact dimensions.

With this program, size reduction efforts were continued to the point where measurements capable of yielding material Hugoniot data can now be made with planar impacts using impacting plates as small as 6 to 12 mm diameter. This size reduction has made possible planar impact experiments for many small ballistic and light-gas gun installations that would not otherwise be employed for such studies.

The initial study has been the impact of copper cylinders into composite materials of copper and polyethylene hot pressed to their theoretical densities. It is designed to test a recently developed theory for establishing the shock properties of a composite mixture by using the properties of the original elements[35].

The experiment was performed on a 13.7 mm (.54 cal.) and a 7.62 mm (.30 cal.) powder gun. A powder gun was chosen in preference to using plate slap for two reasons: (1) the shock wave must be of long duration so that there is no dispersion before it reaches the target rear surface; and (2) the planarity must be accurately controlled. The former is achieved by making the projectile thickness larger than that of the target. The target was placed approximately 3 mm from the muzzle of the gun, so that the one caliber long projectile was still partially in the barrel at impact, thus assuring impact planarity. A modified Beckman & Whitley Model 339 rotating mirror streak camera* was used to observe the plate impact and the resulting rear surface motion of the target. The low pressure rear surface approximation was assumed, i.e., the rear surface velocity is twice the material particle velocity.

Initial results from this study indicate that the pressures generated in the composites are somewhat higher than predicted by theory. The data also suggest that inhomogeneities in the composite materials have introduced measurable scatter into the data.

---

* The modification to the B & W Model 339 Streak Camera is described briefly in Section V of this report.

V. INSTRUMENTATION DEVELOPMENT

The nature of experiments being conducted in all phases of the impact effort require the use of a wide range of time-resolved instrumentation. Instrumentation required for such experiments is either unavailable or is available only at prohibited costs from commercial sources. Accordingly, a significant fraction of the overall effort has been expended upon the development of such instrumentation and, where necessary, upon the generation of computer programs to reduce the raw data. The following is a group of short resumes describing individual systems; more complete descriptions of each system have been published elsewhere and referenced here.

STREAK CAMERA SYSTEMS FOR PRECISE TIME MEASUREMENTS

The majority of time-resolved impact experiments require precise determinations of many times associated with the experimental sequence. Such measurements include initial projectile contact with the target, timing of various x-ray and photo-instrumentation operations, arrival times of shock waves at free surfaces, etc.

High speed chronographs and oscilloscopes are used widely for such measurements but they have high costs per channel of information and cannot be made reliable when employed in large systems. A more satisfactory technique is to employ streak cameras operating in the perpendicular slit mode to view light flashes synchronized with the events of interest. These cameras are almost totally reliable as are many of the systems for synchronizing light flashes with events of interest. In addition, the basic instrumentation system of the facility employs a streak camera for measuring projectile velocity[1]. Swift and Baker[36] reported the introduction of a third slit into a Hall type velocity measurement system that interrupted the light from a series of small xenon flash tubes that were powered by high voltage thyratron circuits. The thyratrons in turn were triggered by electric pulses from the events of interest.

This basic technique has been extended and improved. The most significant improvement was the addition of flash lamps mounted at both ends of each optical slit viewed by the camera[B16]. Simultaneous triggering of these flash lamps allows systematic errors in data reduction due to slit misalignment to be detected and compensated during data reduction. A new group of mechanical-optical transducers have also been developed for use with streak camera systems. These include the scintillation type x-ray burst detector and the interrupted fiber units used to detect shock wave arrival times (both units are described below). Finally, a higher time resolution streak camera (Dynafax Model 319B) has

been used to reduce the minimum resolved time to below 60 ns. Experience at this facility has shown that streak camera time measurement systems are the most reliable available and by far the cheapest when more than four or five of data channels are required. The single disadvantage of streak camera timing systems is the delay between the event and reading the data off processed film. This has not proven to be a problem because of the inherently low data acquisition data rate enforced by ballistic range operation.

X-RAY FLASH DETECTORS

An acute problem with using large arrays of flash x-ray generators for visualizing impact damage as it develops is the reliable determination of the times when each generator is actuated. Internal synchronization pulses are available for time determinations using oscilloscopes or chronographs but multiple x-ray generators require a prohibitively large number of such instruments. Two types of x-ray detectors have been developed that employ part of the actual x-ray beam for time measurements. The first is a planar spark gap[B1] consisting of two sheets of aluminum foil through which the x-ray beam passes on its way to the film (see Figure 34). The gap is stressed to near its breakdown voltage (≈ 10 kV) and x-ray induced ionization of the air in the gap causes it to break down. An associated pulse forming network generates a 10 kV low impedance pulse

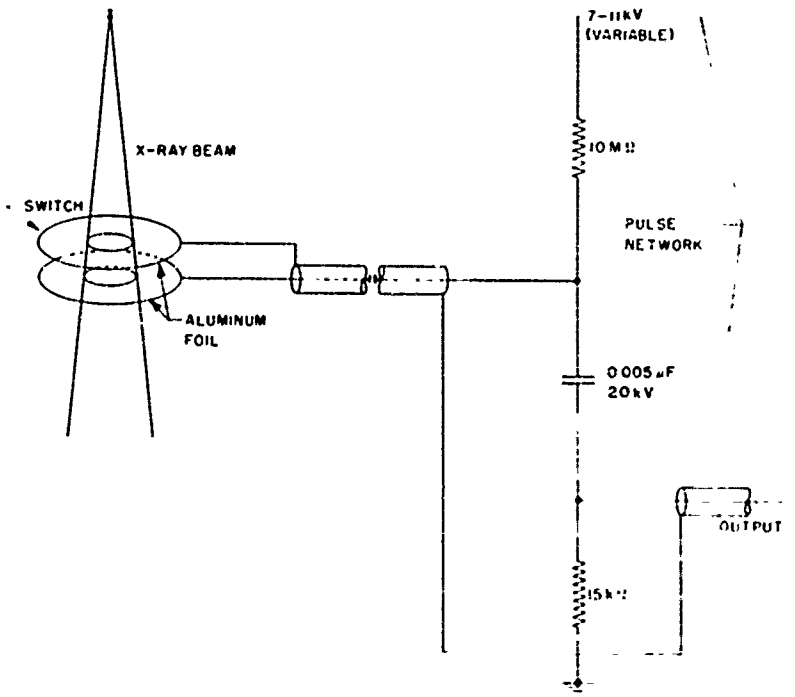

Figure 34. Schematic of Parallel Plate X-ray Triggered Spark Gap Switch.

when the gap is closed. Synchronization between these pulses and the triggering x-ray flash is nearly perfect when the gaps are properly stressed but significant delays (1-10 μsec) are introduced when the stressing voltage is too low. The second type of detector employs a tiny scintillation crystal (thallium doped sodium iodide) to generate an intense flash of blue light when it is irradiated by part of the flash x-ray beam[B17]. The light is conducted to the slit of a medium-speed streak camera with a fiber light guide where it generates an image whose position is proportional to the x-ray firing time. The streak camera has been used to measure the relative times of up to 10 x-ray flashes plus several other optical events. Time resolutions shorter than 60 ns can be achieved routinely. Scintillation crystal detectors possess two important advantages: (1) they have no adjustments; and (2) the resulting signals are compatible with streak camera time measurement systems that are employed widely at the AFML impact facility.

SHOCK ARRIVAL PROBES

Many investigations concerning the dynamics of shock wave interactions require precise time measurements of shock wave arrivals at free surfaces. Pin probes consisting of sharp needles separated from the surface of interest with thin sheets of plastic have been developed for detecting arrivals of strong shock waves. The shock disturbance causes the surface under the needle to recoil, thus pushing the needle through the plastic sheet and discharging a pulse-forming network connected between the needle and the surface.

At somewhat lower peak pressures the leading edges of shock waves develop structures so that different components of the wave arrive at surfaces at slightly different times. Inexpensive piezoelectric probes have been developed for measuring shock wave arrival times by producing electrical signals that are related qualitatively to the pressure time history experienced by material just under the free surface[B18]. Arrival times of various shock components are read from oscilloscope records of the probe signals. The probes consist of thin quartz disks bonded between the surface of interest and short aluminum rods (see Figure 35). The oncoming shock wave propagates through the quartz and into the rod. The probe signal is generated across the quartz crystal, i.e. between the target and the rod. These probes operate effectively at shock pressures up to approximately 50 kb--the pressure level where the crystal is crushed.

A fundamentally new type of shock arrival time probe was developed to the point where feasibility was demonstrated--although no actual results have been gathered with them as yet. Basically, the probes consist of individual optical fibers illuminated at one end with a quasi-continuous source and viewed at the other end with a streak camera. One section of each fiber is placed against the free surface and held in place with a short

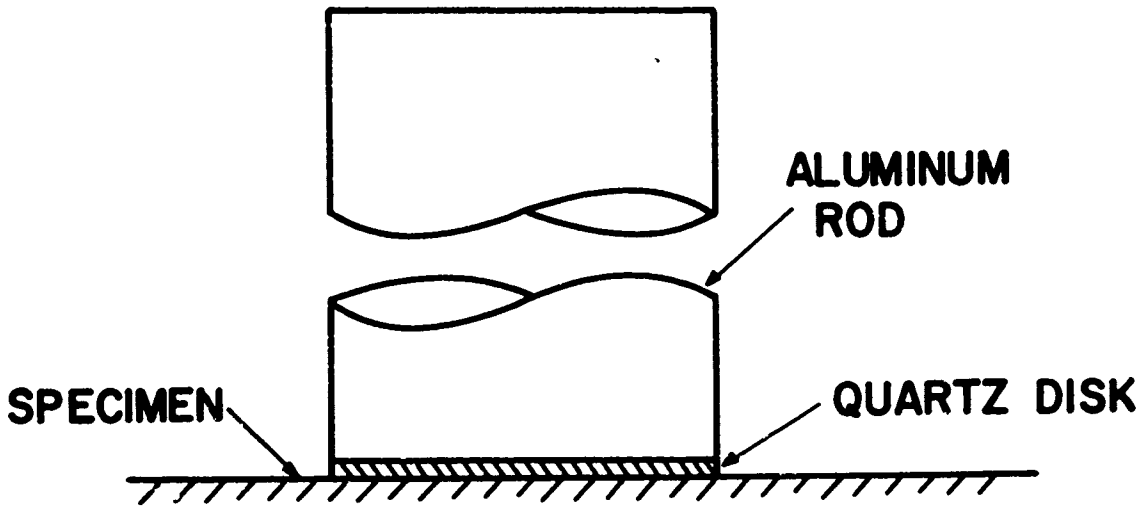

Figure 35. Quartz Piezoelectric Probe.

segment of a razor blade. Shock arrival at the surface forces the fiber against the razor blade severing it. Experience with the fibers indicates that they quit transmitting light long before the blade completes its cut so that their response time is much shorter than originally calculated by assuming the free surface must move one fiber diameter. Systems employing several fibers simultaneously demonstrated that light conducting efficiencies varied substantially enough to require individual balancing if optimum timing accuracies were to be achieved. Present estimates are that up to 100 separate channels could be observed simultaneously with a single streak camera--making such probes the cheapest of any present alternatives when considered on a cost-per-channel basis.

CONVERSION OF A B&W 339 STREAK CAMERA TO GLASS OPTICS

A high performance streak camera (B&W Model 339) was available to the AFML impact facility but fundamental problems with its all-mirror imaging system prevented the camera being used for studies where high optical magnification was required. The mirror imaging system has been replaced with a more conventional lens type imaging system that allows the camera to operate at any desired magnification. In addition, an integral optical bench was installed on the camera that permits the optical slit and all optics in front of it to be moved or interchanged easily. Experience

with the new system indicates that it is both flexible and efficient and can serve most of the requirements imposed by current studies.

SUPER INTENSITY POINT LIGHT SOURCE

The University has discovered that an extended-duration point light source constructed by another AFML contractor[37] has an intensity far in excess of any similar source currently available. The source consists of an enclosed spark gap assembly shown in Figure 36 powered by a 9 kilojoule 20 kV capacitor bank. Effective duration of the light output is controlled stepwise between the limits of 10 and 1000 μsec by adding a tapped inductor to the discharge circuit. Measurements conducted by the University have demonstrated an equivalent black body source temperature of 24,000°K[B14]. Unfortunately, in some cases the fall-time of light energy from the point source exceeds its nominal duration thus complicating its use with continuous-access photographic instrumentation. The University developed a Kerr cell clipper for the source which reduces rise and fall times to less than 100 ns (see Figure 37). The light source has been used successfully with all of the fast cameras at the AFML impact facility.

BALLISTIC PENDULUM FOR MEASURING SMALL VELOCITY SHIFTS

Studies of the interaction between ordnance-velocity projectiles and aircraft structures often require measurements of the velocity loss experienced by projectiles penetrating relatively thin targets. The classic technique for determining such losses is to measure projectile velocity before impact and subtract from it projectile velocity measured after impact. Unfortunately, the precision of such velocity loss determinations becomes very low when the loss itself is low, due to the ancient problem of "small differences between large numbers". A ballistic pendulum was developed which measures such projectile velocity losses directly*. This measurement is accomplished by using the pendulum to measure momentum transferred to the target during an impact and taking proper account of the momenta of debris elements flying away from the impact point[B16].

The pendulum consists of a large wood box with the target mounted at its center. Holes are provided in both ends to allow free passage of the projectile before and after impact. The pendulum is supported with a classic five wire system which allows the box to move laterally without changing its orientation. The large majority of fragments generated by the impact are contained within the pendulum and, thus, do not contribute to its overall momentum change. Results for individual firings are corrected for

---

* The pendulum was developed with the support and guidance of the University by Maj. T. E. Fields as part of his Air Force Institute of Technology Master's Thesis[B28].

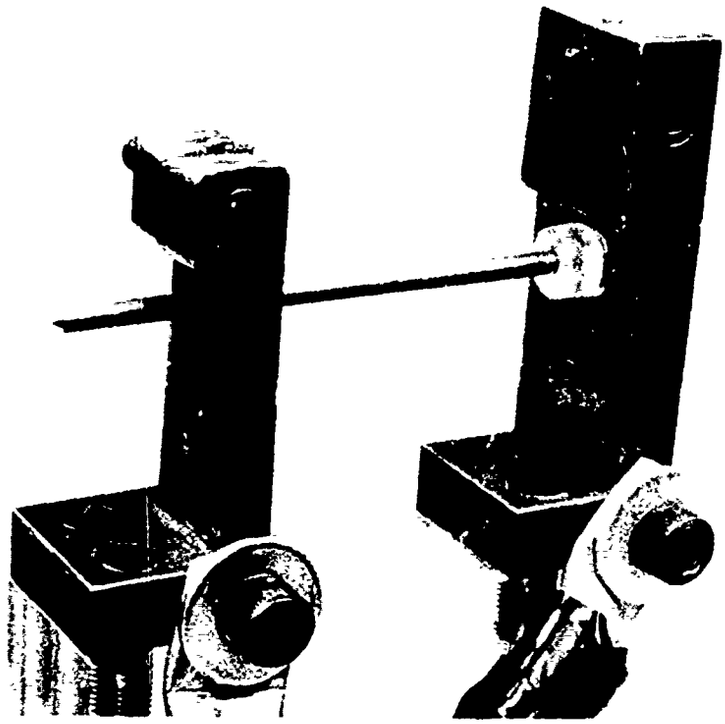

Figure 36. Spark Light Source Assembly.

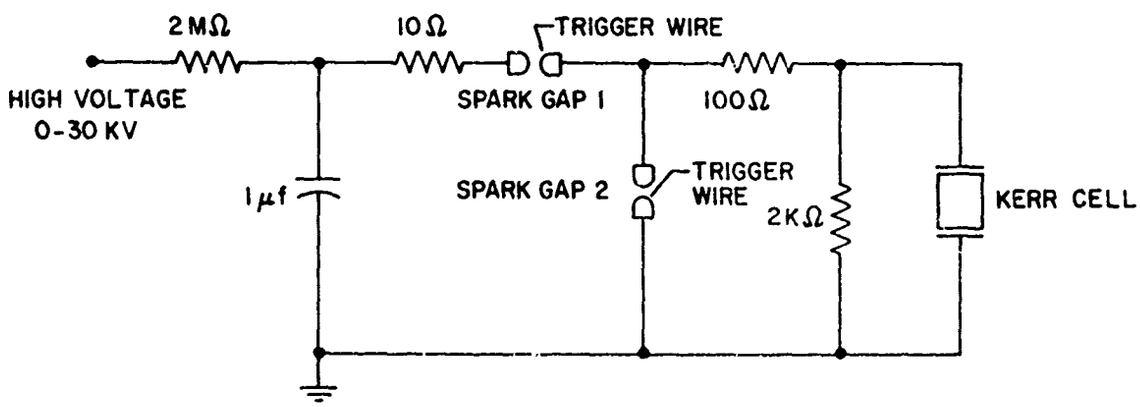

Figure 37. Pulse Forming Network for Kerr Cell Light Clipper.

projectile air drag within the pendulum and for the momenta of any fragments that leave the pendulum (as observed with sequential flash x-rays). Experience with the pendulum system has demonstrated that it can detect projectile velocity shifts as low as 2.5 cm/sec and that its operation is highly reliable.

MOTION ANALYSIS WITH FRAMING CAMERAS

Many studies such as those carried out to characterize impact-induced debris clouds require simultaneous measurements of the velocities and trajectories of many particles or cloud elements. The most efficient technique for carrying out such measurements is to photograph the entire field of interest with an appropriate framing camera and measure the position of each cloud element in each of a sequence of frame images. Knowledge of image position in each frame plus framing rate is sufficient to determine the velocity and trajectory of the element. For proper results, the magnification of each frame and the time between adjacent frames must be known accurately. Initial studies indicated that the highest speed camera available to the facility (B&W 300) is subject to systematic variations of both these parameters[B19]. An intense investigation of these variations led to their evaluations and to a computer program (described below) which automatically compensated for them.

Experience with motion analyses conducted with several cameras has provided much information about ways for setting up experiments, reading the associated film records, and reducing the resulting data to optimize the precision of the final results. The most important single observation is that neither particle velocity nor trajectory can be determined accurately from a single pair of photographs. Proper determinations of these parameters can be made only from a sequence of at least five photographs where statistical techniques can be employed to both minimize and evaluate measurement errors.

DIGITAL MICROSCOPE FOR READING PHOTOGRAPHIC FILMS

Framing camera motion analyses require precise measurements of between 500 and 2000 points on a sequence of photographic images. The total effort required and numerous inevitable mistakes made in measuring this quantity of data by hand with a positional microscope makes such analyses infeasible. Commercial equipment for making such measurements semi-automatically requires investment of between $30,000 and $70,000. The University developed a digital microscope employing a novel technique for digitalizing film position readings that cost under $2,000[B13]. The overall unit shown in Figure 38 projects an enlarged image of the film under investigation onto a screen which contains a fixed position reference (crosshair). The film is moved with the microscope

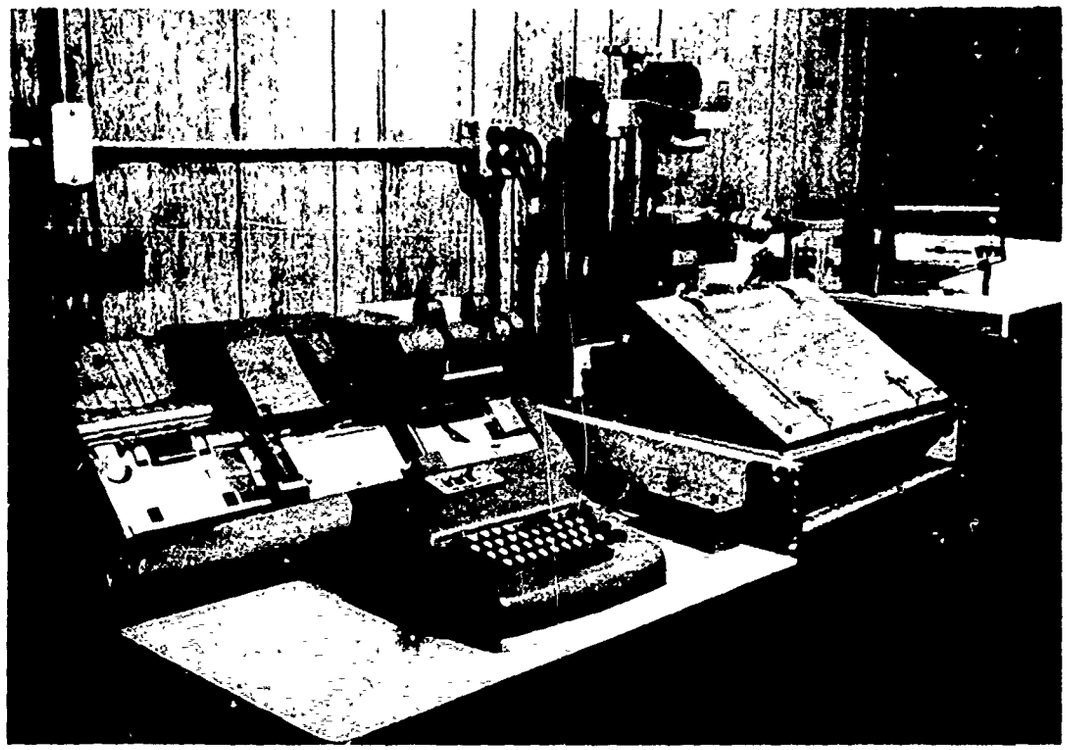

Figure 38. Digital Film Reader System.

stage until the position reference coincides with the desired point and the x and y coordinates of the point are punched onto an IBM card. The microscope has a range of 25 mm x 25 mm with a resolution of better than 25 microns in each direction. An experienced operator can read 2500 to 4000 data points during an eight hour workday. Errors are limited to occasional machine failures and normal interpretation errors.

COMPUTER DATA HANDLING PROGRAMS

Two basic functions are carried out by computer programs. The first is to reduce raw data from film records from a single firing to final form for placing in data books. The second function is to manipulate lists of final data from many experiments to search for correlations, determine trends, produce lists, etc. Several of the major data handling programs are described below; in addition to these programs; small specialized programs have been generated for specific tasks during almost every large experiment. All programs have been written in Fortran IV for use with an IBM 7090/7094 computer system located at Wright-Patterson AFB.

Film Record Programs

Film data that requires processing is obtained from three different types of cameras--streak cameras operating in the perpendicular

slit mode[39], streak cameras operating in the parallel slit mode[39], and framing cameras.

The first of these is represented by the standard Fastax velocity measuring system (described in References 1 and B10) and by a Beckman & Whitley Model 319B drum camera. Relative image positions of these camera records, which are measured to within three microns with a traveling microscope, are directly proportional to elapsed time. By knowing the film speed and the positions, the time between any two images can be determined. The inputs to the Fastax computer program are the positions of the image-events, identifying comments for each image, positions of timing marks on the film, and requests to determine the times between particular pairs of images. The program calculates the film speed, corrects for slit misalignments, determines the time for each event and times between events, calculates the projectile velocity, and prints out this information along with the input information onto a form sized to fit data books. In addition, the program checks critical inputs and prints out warnings if they deviate beyond programmed limits. This basic program has been modified slightly and applied to data from the 319B camera.

Film records from the second class of cameras--streak cameras operating in the parallel slit mode--contain both time and position information. Slopes of line images are directly proportional to object velocities. These records are read on the projection microscope described above which records the x and y position for each point on IBM punch cards. The computer program translates these positions to true location-time coordinates, fits a least square line to them, determines the slope and slope deviation of the line, and prints out the appropriate data including the raw input data and a lineprinter graph of x-t positions of each image. Multiple images can be handled by the program and the input format can be easily modified to accept inputs peculiar to each streak camera (e.g. turbine speed, drum speed, writing rate, etc.).

The third class of cameras--framing cameras--require the most extensive data reduction programs. These programs are designed to follow the x-y positions of many separate items through several frames. Each frame is read individually; first, the coordinates of a fixed fiducial marker and the frame number are punched onto an IBM card, then separate cards are punched to record the coordinates of each item in the frame. This process continues through all frames containing data. Using this data, the computer program calculates true x and y positions of each item in each frame and determines the time for each frame from the frame number. For the B&W 300 camera, these positions and times are corrected for frame-to-frame magnification and framing rate shifts[B19]. Each item then is analyzed separately. Least squares fits of x vs t, y vs t and y vs x are calculated and lineprinter graphs are

printed along with data listings. The deviations of each point and the standard deviation of the fit are also calculated. Experience has shown that points with deviations greater than twice the standard deviation have invariably been caused by reading errors; consequently, they are thrown out automatically and the fit is recalculated. The standard deviation of the slope is determined using the method of Engler[38]. The analysis of each item is terminated with a three-space fit[B49] used to adjust the x-t, y-t, and y-x fits to make them self-consistent. Finally, a summary listing of all items is printed as a single table.

Several variations of the framing camera program are in use. The plate slap facility used only the y-t fit; its program includes bank parameters in the input, and the flyer momentum, planarity, bank efficiency, etc. are listed in the output. The B&W 326B Dynafax framing camera reports times in milliseconds rather than microseconds as do the B&W 300 programs. Other minor variations have also been made from time to time as required by specific experimental situations.

Data Handling Programs

One of the determining factors in the development of new experiments is the availability of previously obtained data that can be applied to the problem at hand. For example, in the hypervelocity program an experiment to correlate projectile velocity with final hole size in thin plates was initiated. A search of our data files revealed that 40% of the experimental data had already been gathered--but in other experiments. This search was facilitated by a computer sorting program containing data from each round. This data includes gun parameters, projectile velocity, and target data written onto magnetic tape. The computer sorting program is quite general; it can sort on several levels and order results according to command so that its output is in an outline format with appropriate headings and subheadings.

Other data handling programs are less general. For example, LABOR* accepts arrays of data points and returns as output a Calcomp graph with the data points plotted and a least squares line (using any one of a number of equation forms) drawn through them; POLYFT is a least squares polynomial fit; and ORIGIN is an extrapolation routine. Many other special single-purpose programs have been written to manipulate data, integrate it, fit it to specific functional relationships, or otherwise transform it to obtain more information or information in a different form.

---

* LABOR is a collection of several subroutines written by the computer staff which were modified and assembled by Maj. R. F. Prater of the Air Force Materials Laboratory.

VI. REFERENCES AND BIBLIOGRAPHY

Sufficient documentation was generated under Contract F33615-68-C-1138 to merit listing it separately in the form of bibliography entries. Bibliography citations are preceeded by a "B". In addition the authors have cited publications generated by this group prior to the current reporting period. These are included in the general references and are cited in the text with plain numbers.

REFERENCES

1. Swift, H. F., "The Air Force Materials Laboratory Hypervelocity Ballistic Range", University of Dayton, Dayton, Ohio, AFML-TR-67-2, Wright-Patterson AFB, Ohio, January 1967 (AD-646,760).

2. Herman, W., and Jones, A. H., "Survey of Hypervelocity Impact Information", Massachusetts Institute of Technology, Aeroelastic and Structures Research Laboratory, Cambridge, Mass., ASRL Report No. 91-1 and Addendum 1, AD-267,289 and AD-267,290, Contract AF19(604)7400, September 1961 and October 1961.

3. Richardson, A. J., "Theoretical Penetration Mechanics of Multisheet Structures Based on Discrete Particle Modeling", North American Rockwell Corporation, Downey, Calif., presented at AIAA Hypervelocity Impact Conference, Cincinnati, Ohio, April 30-May 2, 1969, AIAA Paper 69-371.

4. Frost, V., "Design Methods for Meteoroid Protection", Aerospace Corporation, presented at the OART Meteoroid Impact and Penetration Workshop, Manned Spacecraft Center, Houston, Texas, October 8 and 9, 1968.

5. Maiden, C. J., and McMillan, A. R., "An Investigation of the Protection Afforded a Spacecraft by a Thin Shield", General Motors Corporation, Santa Barbara, Calif., AIAA Journal, 2(11), February 1964, 1992-1998.

6. Halperson, S. M., and Atkins, W. W., "Observations of Hypervelocity Impact", U.S. Naval Research Laboratory, Washington, D. C., 5th Hypervelocity Impact Symposium, Vol. I, Part 2, Colorado School of Mines, Golden, Colorado, April 1962 (AD-284,280).

7. Friend, W. H., et al., "An Investigation of Explosive Oxidations Initiated by Hypervelocity Impacts", Space Research Institute of McGill University, Montreal, Canada, AFFDL-TR-67-92, Wright-Patterson AFB, Ohio, August 1967.

8. Teng, R. N., "Hypervelocity Impact Damage in Cadmium Targets", McDonnell Douglas Corporation, Santa Monica, Calif., Technical Report AFWL-TR-69-134, Kirkland AFB, New Mexico, March 1970.

9. Nysmith, C. R., "An Experimental Impact Investigation of Aluminum Double-Sheet Structures", NASA Ames Research Center, Moffet Field, Calif., AIAA Hypervelocity Impact Conference, Cincinnati, Ohio, April 30-May 2, 1969, AIAA Paper No. 69-375.

10. Swift, H. F., Carson, J. M., and Hopkins, A. K., "Ballistic Limits of 6061-T6 Aluminum Bumper Systems", University of Dayton and Air Force Materials Laboratory, AFML-TR-67-324, Wright-Patterson AFB, Ohio, October 1967 (AD-823, 029).

11. Rolsten, R. F., Wellnitz, J. N., and Hunt, H. H., "An Example of Hole Diameter in Thin Plates Due to Hypervelocity Impact", Journal of Applied Physics, 35 (3), March 1964.

12. Rosenblatt, M., Kreyenhagen, K. N., and Romine, W. D., "Analytical Study of Debris Clouds Formed by Hypervelocity Impacts on Thin Plates", Shock Hydrodynamics, Inc., Sherman Oaks, Calif., AFML-TR-68-266, Wright-Patterson AFB, Ohio, December 1968.

13. Carey, D. A., "An Investigation of the Debris Cloud Produced by the Impact of Spheres on Thin Metal Sheets", Air Force Institute of Technology Master's Thesis No. GSF/Mech 67-1, Wright-Patterson AFB, Ohio, June 1967.

14. Denardo, B. P., Summers J. L., and Nysmith, C. R., "Projectile Size Effects on Hypervelocity Impact Cratering in Aluminum", NASA TN D-4067, Ames Research Center, Moffett Field, Calif., July 1967.

15. Gehring, J. W., "Observations of the Phenomena of Hypervelocity Impact", Ballistic Research Laboratories, Aberdeen Proving Ground, Maryland, 4th Hypervelocity Impact Symposium, Vol. II, APGD-TR-60-39 (II), Eglin AFB, Florida, September 1960 (AD-244, 476).

16. Charest, J. A., "Measurement of Shock Wave Pressures Generated by Hypervelocity Impacts in Aluminum", General Motors Defense Research Laboratory, Santa Barbara, Calif., NASA CR-78399, November 1964 (N66-37523).

17. Billingsley, J. P., "Comparison of Experimental and Predicted Axial Pressure Variation for Metallic Targets Impacted by Metallic Spheres", ARO, Inc., Tullahoma, Tennessee, AEDC-TR-69-49, Arnold Engineering Development Center, Tennessee, July 1969 (AD-69[illegible], 492).

18. Rolsten, R. F., and Hunt, H. H. "Ballistic Behavior of Adhesively Bonded Honeycomb Aluminum Panels for Aircraft: Part II", University of Dayton, Dayton, Ohio, AFML-TR-66-135, Wright-Patterson AFB, Ohio, May 1966 (AD-633, 621).

19. Nishiwaki, J., "Resistance to the Penetration of a Bullet Through Aluminum Plate", Journal of the Physical Society of Japan, 6, October 1961, p. 374-378.

20. Wilkens, M. L., "Third Progress Report of Light Armor Program", Lawrence Radiation Laboratory, University of California, UCRI-50460, July 1968.

21. Duvall, G. E., "Shock Waves in the Study of Solids", Applied Mechanics Review, 15 (11), November 1962, p. 849.

22. Rinehart, J. S., "On Fractures Caused by Explosions and Impacts", Quarterly of the Colorado School of Mines, Golden, Colorado, 55 (4), October 1960.

23. Zeldovich, Ya. B., and Raizer, Yu. P., Physics of Shock Waves and High Temperature Hydrodynamic Phenomena, Chapter II, Academic Press, New York, 1966, translated by J. F. Heyda.

24. van Thiel, M., "Compendium of Shock Wave Data", Lawrence Radiation Laboratory, University of California, Livermore, Calif., UCRL-50108, June 1966.

25. Duvall, G. E., and Fowles, G. R., "Shock Waves", Chapter 9 in High Pressure Physics and Chemistry, Vol. II, edited by R. S. Bradley, Academic Press, New York, 1963, p. 228.

26. Guenther, A. H., "Production of Strong Shocks in Plastics by Ultra-Short Impulsive Loading", AFSWC-TDR-62-125, Kirkland AFB, New Mexico, 1962.

27. Keller, D. V., and Penning, Jr., J. R., "Exploding Foils--The Production of Plane Shock Waves and the Acceleration of Thin Plates" in Exploding Wires, Vol. II, edited by W. G. Chace and H. K. Moore, Plenum Press, New York, 1962, p. 263.

28. Fowles, G. R., "Attenuation of the Shock Wave Produced by a Flying Plate", Journal of Applied Physics, 31 (4), April 1960.

29. Baker, J. R. Maher, W. E., and Swift, H. F., "R. L. C. Circuit Analysis", Memorandum Report No. 1229, U. S. Naval Research Laboratory, Washington, D. C., October 1961 (AD-460, 684).

30. Jajowsky, C., "Spall Studies on 6061-T6 Aluminum", AFWL-TR-69-101, Air Force Weapons Laboratory, Kirkland AFB, New Mexico, September 1969.

31. Meador, J. R., "Revised Sphere-Gap Sparkover Voltages", Transactions of the IEEE, 55, July 1936, p. 783.

32. Skidmore, I. C., "An Introduction to Shock Waves in Solids", Applied Materials Research, 4 (3), July 1965, p. 134.

33. Winch, R. P., Electricity and Magnetism, Prentice Hall, Englewood Cliffs, New Jersey, 1963, p. 111.

34. Craford, F. H., Heat, Thermodynamics, and Statistical Physics, Chapter 7, Barcourt Brace and World, New York, 1963.

35. Torvik, P. J., "Shock Propagation in a Composite Materials", Department of Mechanics, Air Force Institute of Technology, Wright-Patterson AFB, Ohio, accepted by The Journal of Composite Materials, April 1970.

36. Swift, H. F., and Baker, J. R., "Hypervelocity Capability and Impact Research", Semiannual Progress Report, NRL Memorandum Report 1623, U.S. Naval Research Laboratory, Washington, D. C., July 1965.

37. Stevens, H. C., O'Neil, R. W., and Scherrer, V. C., "Development of a Research Capability for Accelerating Hypervelocity Particles", Technical Operations Research, Burlington, Mass., AFML-TR-64-333, Wright-Patterson AFB, Ohio, October 1964.

38. Engler, N. A., "Development of Methods to Determine Winds, Density, Pressure, and Temperature from the ROBIN Falling Balloon", University of Dayton, Dayton, Ohio, UDRI-TR-66-101, AFCRL-65-448, Air Force Cambridge Research Laboratories, Mass., May 1965 (AD-630,200).

39. Hyzer, W. J., Photographic Instrumentation Science and Engineering, U.S. Government Printing Office, Washington, D. C., October 1965.

BIBLIOGRAPHY

Journal Articles

B1. "Flash X-ray Actuated Trigger Swtich", H. F. Swift and E. A. Strader, Review of Scientific Instruments, 39 (5), May 1968, p. 728-730.

B2. "The Effects of Bumper Material Properties on the Operation of Spaced Hypervelocity Particle Shields", H. F. Swift and A. K. Hopkins, Journal of Spacecraft and Rockets, 7 (1), January 1970, p. 73-77.

B3. "Debris Clouds Behind Plates Impacted by Hypervelocity Pellets", H. F. Swift, D. D. Preonas, W. C. Turpin, and Capt. J. M. Carson, Journal of Spacecraft and Rockets, 7 (3), March 1970, pp. 313-318. (This article is from presentation B11.)

B4. "Dissection Methods for Measuring Characteristics of Expanding Clouds", H. F. Swift, D. D. Preonas, and W. C. Turpin, Review of Scientific Instruments, 41 (5), May 1970, pp. 746-751. (This article is based on presentation B15.)

B5. "A Technique for Launching Intermediate Velocity Thin Plastic Sheets", P. W. Dueweke, Review of Scientific Instruments, 41 (4), April 1970, p. 539-541.

Presentations

B6. "Simulation of High Velocity Impacts on Thin Targets", H. F. Swift and Capt. R. F. Prater, OART Meteoroid Impact and Penetration Workshop, Manned Spacecraft Center, October 8-9, 1968, Houston, Texas. (This presentation was based on AFML-TR-68-88, Report B21 and was included in the proceedings.)

B7. "A Study of Ballistic Limits of 6061-T6 Aluminum Bumper Systems and the Role Bumper Materials Play in Overall Shield Effectiveness", Lt. J. M. Carson, A. K. Hopkins, and H. F. Swift, OART Meteoroid Impact and Penetration Workshop, Manned Spacecraft Center, October 8-9, 1968, Houston, Texas. (This presentation was based on AFML-TR-67-324, Ref. 10 and AFML-TR-68-257, report B26, which were included in the proceedings.)

B8. "The Air Force Materials Laboratory Hypervelocity Ballistic Range", H. F. Swift, Aeroballistic Range Association, November 20-21, 1968, Santa Monica, California. (This presentation was based on parts of AFML-TR-67-2, Ref. 1, and was included in the informal proceedings.)

B9. "Simulation of High Velocity Impacts on Thin Targets", H. F. Swift and Capt. R. F. Prater, Aeroballistic Range Association, November 20-21, 1968, Santa Monica, California. (The presentation was based on AFML-TR-68-88, report B21, and was included in the information proceedings.)

B10. "Electro-Optical Clock", H. F. Swift Aeroballistic Range Association, November 20-21, 1968, Santa Monica, California. (This presentation was based on parts of AFML-TR-67-2, Ref. 1, and was included in the informal proceedings.)

B11. "Characterization of Debris Clouds Behind Impacted Meteoroid Bumper Plates", H. F. Swift, D. D. Preonas, Capt. W. C. Turpin, and Capt. J. H. Cunningham, AIAA Hypervelocity Impact Conference, April 30-May 2, 1969, Cincinnati, Ohio. (This presentation was included in the formal proceedings as AIAA Paper 69-380.)

B12. "The Effects of Bumper Material Properties on the Operation of Spaced Hypervelocity Particle Shields", H. F. Swift and A. K. Hopkins, AIAA Hypervelocity Impact Conference, April 30-May 2, 1969, Cincinnati, Ohio. (This presentation was an expansion of AFML-TR-68-257, report B26, and was included in the formal proceedings as AIAA Paper 69-379.)

B13. "An Inexpensive Automatic Digital Film Reader", H. F. Swift, D. D. Preonas, and G. S. Williams, Aeroballistic Range Association, May 12-13, 1969, Ottawa, Canada. (This presentation was included in the informal proceedings.)

B14. "High Intensity Point Light Source", D. D. Preonas and H. F. Swift, Aeroballistic Range Association, May 12-13, 1969, Ottawa, Canada. (This presentation was included in the informal proceedings.)

B15. "D ssection Methods for Measuring the Characteristics of Expanding Clouds", H. F. Swift, D. D. Preonas, and W. C. Turpin, Aeroballistic Range Association, November 3-6, 1969, Dayton, Ohio. (This presentation was included in the informal proceedings.)

B16. "Ballistic Pendulum for Measuring Small Shifts in Projectile Velocities", H. F. Swift, R. S. Bertke, and Maj. T. E. Fields, Aeroballistic Range Association, November 3-6, 1969, Dayton, Ohio. (This presentation was included in the informal proceedings.)

B17. "Recording Flash X-ray Burst Times With Scintillation Crystals", H. R. Taylor, D. D. Preonas, and H. F. Swift, Aeroballistic Range Association, November 3-6, 1969, Dayton, Ohio. (This presentation was included in the informal proceedings.)

B18. "Piezoelectric Shock Wave Arrival Time Sensor", Maj. R. F. Prater, H. R. Taylor, and H. F. Swift, Aeroballistic Range Association, November 3-6, 1969, Dayton, Ohio. (This presentation was included in the informal proceedings.)

B19. "Quantitative Motion Analysis from Rotating Mirror Framing Camera Records", D. D. Preonas and Maj. R. F. Prater, Aeroballistic Range Association, November 3-6, 1969, Dayton, Ohio. (This presentation was included in the informal proceedings.)

Reports

B20. "A Diameter Gage for True Stress-True Strain Measurements of Tensile Specimens at Reduced Temperatures", I. B. Fiscus and Lt. J. M. Carson, AFML-TR-68-27, February 1968 (AD-669, 848).

B21. "Simulation of High Velocity Impacts on Thin Sheets", H. F. Swift and Capt. R. F. Prater, AFML-TR-68-88, May 1968 (AD-671, 522).

B22. "Momentum Distribution in the Debris Cloud Produced by Hypervelocity Perforation of Thin Plates", Capt. J. H. Cunningham, AFML-TR-68-174, July 1968 (AD-674, 592). (AFIT Master's Thesis GSF/MC/68-4)

B23. "Investigation of Crater Growth and Ejecta Cloud Resulting from Hypervelocity Impact of Aluminum Spheres on Thick Aluminum Targets", Lt. Col. R. H. Smith, AFML-TR-68-175, June 1968 (AD-673, 515). (AFIT Master's Thesis GSF/MC/68-10.)

B24. "Evaluation of Small Arms Impact on F-111 Aircraft Bonded Aluminum Honeycomb Panels", F. J. Roth, AFML-TR-68-224, July 1968 (AD-843, 216L).

B25. "Some Properties of Iron, Copper, and Selected Aluminum Alloys Including True Stress-True Strain at Reduced Temperatures". Lt. J. M. Carson and J. M. Hawn, AFML-TR-68-251, September 1968 (AD-676, 705).

B26. "The Effects of Bumper Material Properties on the Operation of Spaced Hypervelocity Particle Shields", H. F. Swift and A. K. Hopkins, AFML-TR-68-257, September 1968 (AD-676, 275).

B27. "AFML Electrical Plate Slap Facility", D. D Preonas, AFML-TR-68-352, November 1968 (AD-685, 189).

B28. "The Effect of Projectile Shape on the Ballistic Perforation of Thin Armor Plate", Maj. T. E. Fields, AFML-TR-69-202, July 1969 (AD-693, 151). (AFIT Master's Thesis GAW/MC/69-2.)

B29. "Hypervelocity Perforation Mechanics of Thin Metal Plates", W. C. Turpin, AFML-TR-69-203, July 1969 (AD-693, 210). (AFIT Master's Thesis GSF/MC/68-12.)

B30. "The Air Force Materials Laboratory Terminal Ballistic Research Facility", R. S. Bertke, AFML-TR-69-215, August 1969.

B31. "AFML Electric Plate Slap Facility", P. W. Dueweke and D. D. Preonas, AFML-TR-70-28, April 1970. (in press)

B32. "Hole Growth in Thin Plates Perforated by Hypervelocity Pellets", W. C. Turpin and Capt. J. M. Carson, AFML-TR-70-83, April 1970.

B33. "Characterization of Debris Clouds Behind Impacted Meteoroid Bumper Plates", H. F. Swift, D. D. Preonas, W. C. Turpin, and Capt. J. M. Carson, in preparation (this is a considerable expansion of article B3).

Technical Memoranda

B34. "Hole Diameters in Thin Plates Perforated by Hypervelocity Projectiles", Lt. J. M. Carson and H. F. Swift, AFML/MAY-TM-67-9, November 1967.

B35. deleted

B36. "Round Robin Series No. 1", M. F. Lehman, HV-68-4, 2 December 1969.

B37. "Digital Voltmeter Bank Voltage Monitor", P. W. Dueweke, HV-69-1, 2 January 1969.

B38. "Plate Slap Voltage--Velocity Composite", P. W. Dueweke, HV-69-4, 13 January 1969.

B39. "Spall Threshold Study of Ceramic", P. W. Dueweke, HV-69-15, 14 January 1969.

B40. "Residual Strength of Honeycomb Panels After .50 API Impacts", R. S. Bertke, UDRI-TM-69-03, February 1969.

B41. "Residual Strength and Damage to Chem-Milled Sheet Panels After Impacts With .30-06 and .50-Caliber Projectiles", R. S. Bertke, UDRI-TM-69-02, February 1969.

B42. "Comparison of Results on Boron Panels With Unmilled and Chem-Milled Aluminum Sheet Panels After an Impact With a .30-06 Caliber Projectile", R. S. Bertke, UDRI-TM-69-16, November 1969.

B43. "Ballistic Limit Study of CS/0-0-P1-400-s1 Style .400" Ballistic Felt, 51 oz. sq. yd.", M. F. Lehman, HV-69-23, 28 March 1969.

B44. "Ballistic Study of Parachute Back Pack B5-MA1", M. F. Lehman, HV-69-24, 28 March 1969.

B45. "Ultimate and Impact Tests on Fiberglass Panels", R. S. Bertke, UDRI-TM-69-05, May 1969.

B46. "JIBAC Round Robin Test, Phase II", M. F. Lehman, HV-69-42, 2 June 1969.

B47. "Impact Tests on Boron-Epoxy Panels", R. S. Bertke, UDRI-TM-69-10, August 1969.

B48. "Comparison of Ballistic Limits for Laminated 1100 Aluminum Plates With Similar Homogeneous Aluminum Plates", M. F. Lehman, HV-69-50, 9 July 1969.

B49. "Three-Space Fit Calculations for Film Reader Programs", D. D. Preonas, HV-69-53, 8 August 1969.

B 50. deleted.

B51. "Damage Received by Steel Plate Impacted by Depleted Uranium Projectile", J. E. Green, C. E. Acton, and R. S. Bertke. HV-69-68, 28 October 1969.

B52. "Relationship of Residual Strength of Aluminum Specimens With Drilled Holes to Specimens With .30-60 Caliber Projectiles", J. E. Green, C. E. Acton, and R. S. Bertke, UDRI-TM-69-15, November 1969.

B 53. deleted.

E54. "Preliminary Damage Threshold Study of Boron Nitride", P. W. Dueweke, HV-69-77, 5 December 1969.

B55. "Damage Received by (Honeycomb Sandwiched Between Two Boron Skins) Panels Impacted by .50 AP-M2 Caliber Projectiles", R. S. Bertke, C. E. Acton, and J. E. Green, HV-69-78, 9 December 1969.

B.56 and B 57 deleted.

B58. "Ballistic Limit Established by Caliber .30 AP-M2 Impact Tests on Ceramic Armor With Graphite Reinforcement Backing Material", R. S. Bertke, C. E. Acton, and J. E. Green, HV-70-8, 9 February 1970.

B59. "Thermal and Acoustic Properties of Blanket-Type Candidate Materials", R. S. Bertke, UDRI-TM-69-13, 27 October 1969.

B60. "Response of Materials to Pulse Loads", H. F. Swift, University of Dayton Research Institute, Dayton, Ohio, Technical Management Reports, Contract F33615-68-C-1138: UDRI-QPR-68-08, May 1968; UDRI-QPR-68-11, November 1968; UDRI-QPR-69-02, May 1969; UDRI-QPR-69-12, December 1969.